

SPATIAL SCALE SEPARATION AND EMERGENT PATTERNS IN COUPLED DIFFUSIVE–NONDIFFUSIVE SYSTEMS

THÉO ANDRÉ  , SZYMON CYGAN  , ANNA MARCINIAK-CZUCHRA  ,
AND FINN MÜNNICH 

ABSTRACT. This paper investigates pattern formation in reaction–diffusion systems with both diffusive and nondiffusive components, establishing the existence of far-from-equilibrium patterns and providing necessary and sufficient conditions for diffusion-driven instability (DDI). In particular, we prove the existence of far-from-equilibrium patterns exhibiting branch-switching and discontinuities in the nondiffusive components, which cannot occur in classical reaction–diffusion equations. While previous work has linked DDI to instability in the purely nondiffusive subsystem – thereby destabilizing all regular Turing patterns – we show that DDI can also arise from subsystems involving nondiffusive and slow-diffusive components. This leads to simple sufficient conditions for DDI in systems with arbitrary numbers of components. Further, we fully classify all possible sources of DDI in the case of two diffusive and one nondiffusive component, illustrating our results with a receptor-based model supported by numerical bifurcation analysis and simulations. These findings extend the theoretical foundations of pattern formation, demonstrating how coupling between diffusive and nondiffusive dynamics can generate patterns beyond the reach of the classical reaction-diffusion framework.

1. INTRODUCTION

Reaction–diffusion systems provide a foundational framework for understanding self-organized pattern formation in biological, chemical, and ecological contexts. While classical Turing theory predicts patterns through diffusion-driven instability (DDI), experimental identification of the diffusive components required for such mechanisms remains limited. Many biological systems, however, involve nondiffusive, spatially localized components—such as membrane-bound receptors or intracellular signaling molecules—that are not captured by standard reaction–diffusion models. Perturbations of these nondiffusive components can significantly influence pattern formation, motivating the study of coupled reaction–diffusion–ODE systems.

In such models, only a subset of variables diffuses, reflecting spatially localized dynamics [10, 12, 13, 18, 19, 25, 26]. Examples include receptor-based models in developmental biology, where diffusive ligands mediate cell-to-cell communication while intracellular signaling remains localized. These models have been rigorously derived from microscopic descriptions via homogenization [20, 22], providing a sound mathematical basis for their use.

Coupling nondiffusive components with diffusive species introduces spatial scale separation, which fundamentally alters the system’s dynamics. Traditional pattern formation analysis typically focuses on near-equilibrium Turing mechanisms, but the presence of nondiffusive components can lead to irregular or singular structures, such as jump discontinuities or spike patterns, characteristic of far-from-equilibrium behavior [1, 6, 9, 10, 11, 14, 21].

The first contribution of this work is a proof of existence for a class of far-from-equilibrium patterns that arise independently of diffusion-driven instability and do not occur in classical

Key words and phrases. Reaction-diffusion equation, pattern formation, diffusion-driven instability, discontinuous steady states.

reaction–diffusion systems. In some cases, when Turing patterns are unstable, trajectories may approach these far-from-equilibrium structures.

The second contribution is the derivation of sufficient conditions for DDI in general reaction–diffusion–ODE systems with an arbitrary number of components. While destabilization by the ODE subsystem can trigger DDI, it inherently destabilizes all classical Turing patterns [5], motivating the identification of alternative mechanisms. We show that DDI can arise from the interplay of nondiffusive and slow-diffusive components, and, in some cases, from subsystems involving fast-diffusing and slow-diffusing species.

The paper is structured as follows. Section 2 introduces the general reaction–diffusion–ODE framework. Section 3 proves the existence of far-from-equilibrium patterns. Section 4 presents sufficient conditions for DDI in systems with arbitrary number of components. Section 5 analyzes a three-component system in detail, illustrating patterns arising from two-stage spatial scale separation. Section 6 applies these results to a receptor-based model, highlighting new insights into pattern formation in biological systems such as Hydra morphogenesis.

2. MATHEMATICAL SETTING

We consider a coupled reaction–diffusion–ODE system with $m = m_u + m_v + m_w$ components of the form

$$(1) \quad \begin{cases} \partial_t u = f(u, v, w), \\ \partial_t v = D_v \Delta v + g(u, v, w), \\ \partial_t w = D_w \Delta w + h(u, v, w) \end{cases}$$

posed in a bounded domain $\Omega \subset \mathbb{R}^n$ with Lipschitz boundary. Here, u denotes the m_u non-diffusing components, v the m_v slow-diffusing components, and w the m_w fast-diffusing components. The diffusion matrices D_v and D_w are diagonal with strictly positive entries, while the non-diffusing components have vanishing diffusion. Homogeneous Neumann boundary conditions are imposed on all diffusive species.

Let $F = (f, g, h)$ denote the reaction terms, assumed to be at least C^2 ; weaker regularity suffices for our main results [16]. The system can be linearized around a steady state $\tilde{X} = (\tilde{u}, \tilde{v}, \tilde{w})$ as

$$\begin{aligned} \partial_t \xi &= \mathcal{L} \xi + \mathcal{N}(\xi), \\ \xi(0) &= \xi^0, \end{aligned}$$

where $D := \text{diag}(0, D_v, D_w)$ is the diffusion matrix, $J := \nabla_{(u,v,w)} F(\tilde{X})$ is the Jacobian at the steady state, ξ denotes the perturbation, \mathcal{L} the linearized operator, and $\mathcal{N}(\xi)$ collects higher-order terms.

A constant steady state $\tilde{X} = (\bar{u}, \bar{v}, \bar{w})$ undergoes diffusion-driven instability (DDI) if it is stable in the corresponding ODE system ($D_v = D_w = 0$) but loses stability when diffusion is introduced. For reaction–diffusion–ODE models, nonlinear (in)stability of a bounded steady state follows directly from its linear (in)stability [16, Theorems 3.3 and 3.7]. Linear stability reduces to the spectral analysis of the operator $\mathcal{L} = D\Delta + J$, with spectral bound $s(\mathcal{L}) = \sup_{\lambda \in \sigma(\mathcal{L})} \text{Re } \lambda$. For a bounded steady state \tilde{X} , the spectrum of \mathcal{L} can be decomposed as

$$(2) \quad \sigma(\mathcal{L}) = \sigma(\nabla_u f(\tilde{X})) \cup \sigma_p(\mathcal{L}),$$

under the assumption $D_v, D_w > 0$ [15, Section 5.22], [16, Proposition 2.3]. In the case of a constant steady state \tilde{X} , the point spectrum is expressed in terms of the eigenvalues $(\lambda_j)_{j \geq 0}$ of

the Laplace operator $-\Delta$ with Neumann boundary conditions:

$$(3) \quad \sigma_p(\mathcal{L}) = \bigcup_{j=0}^{\infty} \sigma(-\lambda_j D + J) = \bigcup_{j=0}^{\infty} \{ \lambda \in \mathbb{C} \mid \det(\lambda I + \lambda_j D - J) = 0 \}.$$

For later reference, we define the following submatrices of $J = \nabla_{(u,v,w)} F(\bar{X})$:

$$(4) \quad \begin{aligned} J_1 &:= \nabla_u f(\bar{X}) \in \mathbb{R}^{m_u \times m_u}, \quad J_2 := \nabla_v g(\bar{X}) \in \mathbb{R}^{m_v \times m_v}, \quad J_3 := \nabla_w h(\bar{X}) \in \mathbb{R}^{m_w \times m_w}, \\ J_{12} &:= \nabla_{(u,v)}(f, g)(\bar{X}) = \begin{pmatrix} \nabla_u f(\bar{X}) & \nabla_v f(\bar{X}) \\ \nabla_u g(\bar{X}) & \nabla_v g(\bar{X}) \end{pmatrix} \in \mathbb{R}^{(m_u+m_v) \times (m_u+m_v)}, \\ J_{13} &:= \nabla_{(u,w)}(f, h)(\bar{X}) = \begin{pmatrix} \nabla_u f(\bar{X}) & \nabla_w f(\bar{X}) \\ \nabla_u h(\bar{X}) & \nabla_w h(\bar{X}) \end{pmatrix} \in \mathbb{R}^{(m_u+m_w) \times (m_u+m_w)}, \\ J_{23} &:= \nabla_{(v,w)}(g, h)(\bar{X}) = \begin{pmatrix} \nabla_v g(\bar{X}) & \nabla_w g(\bar{X}) \\ \nabla_v h(\bar{X}) & \nabla_w h(\bar{X}) \end{pmatrix} \in \mathbb{R}^{(m_v+m_w) \times (m_v+m_w)}. \end{aligned}$$

3. EXISTENCE OF FAR-FROM-EQUILIBRIUM PATTERNS

We now prove the existence of nonconstant stationary solutions to the reaction–diffusion–ODE system (1) consisting of a nondiffusive block \tilde{u} and diffusive components (\tilde{v}, \tilde{w}) , posed in a bounded C^2 –domain $\Omega \subset \mathbb{R}^n$ with homogeneous Neumann boundary conditions. The stationary problem reads

$$(5) \quad \begin{cases} 0 = f(\tilde{u}, \tilde{v}, \tilde{w}), \\ 0 = D_v \Delta \tilde{v} + g(\tilde{u}, \tilde{v}, \tilde{w}), \\ 0 = D_w \Delta \tilde{w} + h(\tilde{u}, \tilde{v}, \tilde{w}), \end{cases}$$

with $D_v > 0$, $D_w > 0$ the diffusion coefficients of slow and fast components, respectively. We aim for *far-from-equilibrium* patterns, i.e., stationary solutions differing from a constant steady state on a set of positive measure. The construction follows the method in [6], adapted to our general PDE–ODE setting.

3.1. Two-branch structure in the \tilde{u} –nullcline. Let $\bar{X} = (\bar{u}, \bar{v}, \bar{w}) \in \mathbb{R}^m$ denote a constant solution of (5) with Jacobian J with submatrices as in (4).

Assumption 3.1. *The linearization matrices satisfy*

$$\det J_1 \neq 0 \quad \text{and} \quad \det(J - D\lambda_j) \neq 0 \quad \text{for all Neumann eigenvalues } \lambda_j \text{ of } -\Delta \text{ on } \Omega.$$

This ensures that the implicit function theorem applies to $f(\cdot, v, w) = 0$, yielding a C^2 map

$$\varphi : \mathcal{V} \times \mathcal{W} \rightarrow \mathbb{R}^{m_u}, \quad \varphi(\bar{v}, \bar{w}) = \bar{u}, \quad f(\varphi(v, w), v, w) = 0,$$

for (v, w) in a neighborhood $\mathcal{V} \times \mathcal{W}$ of (\bar{v}, \bar{w}) . The key ingredient for our construction is the existence of *multiple distinct solution branches* for the equation $f(u, v, w) = 0$ with respect to the nondiffusive variable u , all defined on the same domain $\mathcal{V} \times \mathcal{W} \subseteq \mathbb{R}^{m_u}$.

Assumption 3.2 (Two distinct branches). *There exist two distinct C^2 –maps $\varphi, \psi : \mathcal{V} \times \mathcal{W} \rightarrow \mathbb{R}^{m_u}$ with*

$$f(\varphi(v, w), v, w) = f(\psi(v, w), v, w) = 0,$$

$$\varphi(\bar{v}, \bar{w}) = \bar{u} \text{ and } \varphi \neq \psi \text{ on } \mathcal{V} \times \mathcal{W}.$$

These form two branches of the \tilde{u} -nullcline and allow constructing stationary solutions of (1) that switch between them.

3.2. Elliptic regularity for the diffusive block. We first establish uniform $W^{2,p}$ bounds for the diffusive subs.

Lemma 3.3. *Let $\partial\Omega$ be of class C^2 and fix $p \in [2, \infty)$. Let $D^d \in \mathbb{R}^{m_d \times m_d}$ be diagonal and $J \in \mathbb{R}^{m_d \times m_d}$ satisfying $\det(J - D^d \lambda_j) \neq 0$ for all $j \in \mathbb{N}_0$. Then, for each $\zeta \in L^p(\Omega)^{m_d}$, the problem*

$$(6) \quad D^d \Delta \nu + J \nu = \zeta \text{ in } \Omega, \quad \partial_n \nu = 0 \text{ on } \partial\Omega$$

admits a unique weak solution $\nu \in W^{2,p}(\Omega)^{m_d}$ with

$$(7) \quad \|\nu\|_{W^{2,p}(\Omega)} \leq C \|\zeta\|_{L^p(\Omega)}.$$

Proof. The case $p = 2$ follows from classical existence and $W^{2,2}$ -regularity theory for elliptic problems [8, Theorem 2.4.1.3]. Our system framework allows us to extend this result since the solution to equation (6) can be expressed through the explicit representation

$$\nu = \sum_{j=0}^{\infty} \left(J - D^d \lambda_j \right)^{-1} \begin{pmatrix} \langle \zeta_1, e_j \rangle e_j \\ \vdots \\ \langle \zeta_{m_d}, e_j \rangle e_j \end{pmatrix}$$

where e_j denotes the eigenfunction associated with eigenvalue λ_j . This directly yields $\nu \in W^{2,2}(\Omega)^{m_d}$ and establishes inequality (7) for $p = 2$.

To handle the case $p > 2$, we reformulate equation (6) component-wise as

$$(D^d \Delta - I) \nu_j = \zeta_j + \nu_j - \sum_{i=1}^{m_d} J_{ij} \nu_i \quad \text{for each } j \in \{1, \dots, m_d\}.$$

Employing L^p -regularity theory (cf. [17, Thm 3.1.3]), the Sobolev embedding $W^{2,2}(\Omega) \subseteq L^p(\Omega)$ for $p \in (1, \infty)$ when $n \leq 4$ and for $p \in (2, 2n/(n-4))$ when $n > 4$, combined with inequality (7) applied to each component, we derive

$$(8) \quad \begin{aligned} \|\nu_j\|_{W^{2,p}(\Omega)} &\leq C \left(\|\zeta\|_{L^p} + \sum_{j=1}^{\infty} \|\nu_j\|_{L^p} \right) \\ &\leq C \left(\|\zeta\|_{L^p} + \sum_{j=1}^{\infty} \|\nu_j\|_{W^{2,2}} \right) \leq C \|\zeta\|_{L^p}. \end{aligned}$$

The extension to the complete range $p \in [2, \infty)$ follows by iterating this bootstrap procedure on inequality (8), utilizing the Sobolev embedding $W^{2,p} \subseteq L^q$ with $q < np/(n-2p)$, which confirms that inequality (7) holds throughout this range. \square

3.3. Localised branch switching. We now state a perturbation lemma allowing different reaction terms on two complementary subdomains.

Lemma 3.4. *Let $p > n/2$, $p \geq 2$ and $q_1, q_2 \in C_b^2(\mathbb{R}^{m_d}, \mathbb{R}^{m_d})$ (i.e. all derivatives up to order two are bounded). Assume that for some $\bar{v} \in \mathbb{R}^{m_d}$ we have*

$$q_1(\bar{v}) = 0 \quad \text{and} \quad \det(\nabla_\nu q_1(\bar{v}) - D\lambda_j) \neq 0 \quad \text{for each } j \in \mathbb{N}_0.$$

Then, there exists $\varepsilon_0 > 0$ and, for $\varepsilon \in (0, \varepsilon_0)$, a $\delta > 0$ such that for any open subset $\Omega_1 \subset \Omega$ with $\Omega_2 = \Omega \setminus \overline{\Omega_1}$ and $|\Omega_2| \leq \delta$, the problem

$$(9) \quad D\Delta \nu + q_1(\nu) \mathbb{1}_{\Omega_1} + q_2(\nu) \mathbb{1}_{\Omega_2} = 0 \quad \text{in } \Omega$$

admits a weak solution $\nu \in W^{2,p}(\Omega)^{m_d}$ with $\|\nu - \bar{v}\|_{W^{2,p}(\Omega)} \leq \varepsilon$.

Proof. By mapping $v \rightarrow v + \bar{v}$, $q_1(v) \rightarrow q_1(v + \bar{v})$ and $q_2(v) \rightarrow q_2(v + \bar{v})$, we may assume without loss of generality that $\bar{v} = 0$. We write equation (9) in the equivalent form

$$(10) \quad \begin{aligned} \nu &= (D\Delta + \nabla_\nu q_1(0))^{-1} \left((\nabla_\nu q_1(0)\nu - q_1(\nu)) \mathbb{1}_{\Omega_1} \right) \\ &\quad + (D\Delta_\nu + \nabla_\nu q_1(0))^{-1} \left((\nabla_\nu q_1(0)\nu - q_2(\nu)) \mathbb{1}_{\Omega_2} \right) \\ &= \mathcal{T}_1(\nu) + \mathcal{T}_2(\nu). \end{aligned}$$

By Lemma 3.3 the operator $(D\Delta + \nabla_\nu q_1(0))^{-1}$ with $J = \nabla_\nu q_1(0)$ satisfies the estimate

$$(11) \quad \left\| (D\Delta + \nabla_\nu q_1(0))^{-1} \zeta \right\|_{W^{2,p}} \leq C \|\zeta\|_{L^p(\Omega)}$$

for each $p \geq 2$ and all $\zeta \in L^p(\Omega)^{m_d}$. Our goal is to show that the right-hand side of equation (10) defines a contraction on the ball

$$B_\varepsilon(0) = \left\{ \nu \in W^{2,p}(\Omega)^{m_d} : \|\nu\|_{W^{2,p}} \leq \varepsilon \right\}$$

provided $|\Omega_2|$ and $\varepsilon > 0$ are sufficiently small.

First, we deal with the operator \mathcal{T}_1 . Since $q_1 \in C_b^2(\mathbb{R}^{m_d}, \mathbb{R}^{m_d})$ and $q_1(0) = 0$ by the Taylor expansion we get

$$\left| \nabla_\nu q_1(0)\nu(x) - q_1(\nu(x)) \right| \leq \left| \frac{1}{2} \sum_{j,l=1}^k \partial_{\nu_i \nu_j} q_1(0) \nu_j(x) \nu_l(x) \right| \leq C |\nu(x)|^2,$$

where $|\nu|$ denotes the euclidean norm of a vector $\nu(x) \in \mathbb{R}^k$. Hence, by estimate (11) and the Sobolev embedding $W^{2,p}(\Omega) \subseteq L^\infty(\Omega)$ for $p > N/2$, there exists a constant $C > 0$ such that for each $\nu \in B_\varepsilon(0)$ we have

$$(12) \quad \|\mathcal{T}_1(\nu)\|_{W^{2,p}} \leq C \|\nu(\cdot)|^2\|_{L^\infty(\Omega)} \leq C \|\nu\|_{L^\infty(\Omega)}^2 \leq C \varepsilon^2.$$

Analogously, by the Taylor expansion,

$$\begin{aligned} &\left| \nabla_\nu q_1(0)\nu(x) - q_1(\nu(x)) - \left(\nabla_\nu q_1(0)\omega(x) - q_1(\omega(x)) \right) \right| \\ &\leq |q_1(\nu(x)) - q_1(\omega(x)) + \nabla_\nu q_1(\omega(x))(\nu(x) - \omega(x))| \\ &\quad + |(\nabla_\nu q_1(\omega(x)) - \nabla_\nu q_1(0))(\nu(x) - \omega(x))| \\ &\leq \frac{1}{2} \|\nabla_\nu^2 q_1\|_{L^\infty} |\nu(x) - \omega(x)|^2 + \|\nabla_\nu q_1\|_{L^\infty} |\omega(x)| |\nu(x) - \omega(x)|. \end{aligned}$$

Hence, as in inequalities (12), for $\nu, \omega \in B_\varepsilon(0)$, we obtain

$$(13) \quad \|\mathcal{T}_1(\nu) - \mathcal{T}_1(\omega)\|_{W^{2,p}} \leq C \varepsilon \|\nu - \omega\|_{W^{2,p}(\Omega)}.$$

Here, we choose $\varepsilon_0 > 0$ such that for all $\varepsilon \in (0, \varepsilon_0)$ it holds

$$C \varepsilon^2 \leq \varepsilon/2 \quad \text{and} \quad C \varepsilon < 1/2.$$

This gives is the wanted estimates in equations (12) and (13).

Now we turn to the operator \mathcal{T}_2 . We begin by the following inequality

$$(14) \quad |\nabla_\nu q_1(0)\nu(x) - q_2(\nu(x))| \leq \|\nabla_\nu q_1\|_{L^\infty} |\nu(x)| + \|q_2\|_{L^\infty}.$$

Thus, by estimate (14) and the embedding $W^{2,p}(\Omega) \subseteq L^\infty(\Omega)$ for $p > N/2$, for each $\nu \in B_\varepsilon(0)$ we get

$$(15) \quad \begin{aligned} \|\mathcal{T}_2(\nu)\|_{W^{2,p}} &\leq C \left(\|\nabla_\nu q_1\|_{L^\infty} \|\nu \cdot \mathbb{1}_{\Omega_2}\|_{L^p} + \|q_2\|_{L^\infty(\mathbb{R})} \|\mathbb{1}_{\Omega_2}\|_{L^p} \right) \\ &\leq C |\Omega_2|^{\frac{1}{p}} \left(\|\nu\|_{W^{2,p}} + 1 \right). \end{aligned}$$

Analogously, we have

$$(16) \quad \begin{aligned} & \left| \nabla_\nu q_1(0)\nu(x) - q_2(\nu(x)) - (\nabla_\nu q_1(0)\omega(x) - q_2(\omega(x))) \right| \\ & \leq \left(\|\nabla_\nu q_1(0)\|_{L^\infty} + \|\nabla_\nu q_2(0)\|_{L^\infty} \right) |\nu(x) - \omega(x)|. \end{aligned}$$

Thus, by inequality (16), as in estimate (15), for $v, w \in B_\varepsilon(0)$, we obtain

$$(17) \quad \begin{aligned} \|\mathcal{T}_2(\nu) - \mathcal{T}_2(\omega)\|_{W^{2,p}} & \leq C \|(\nu - \omega) \mathbb{1}_{\Omega_2}\|_{L^p(\Omega)} \\ & \leq C |\Omega_2|^{\frac{1}{p}} \|\nu - \omega\|_{W^{2,p}}. \end{aligned}$$

Here, we choose $\delta > 0$ such that for $\Omega_2 \subseteq \mathbb{R}^N$ satisfying $|\Omega_2| < \delta$ we have

$$C(\varepsilon + 1) |\Omega_2|^{\frac{1}{p}} \leq \varepsilon/2 \quad \text{and} \quad C |\Omega_2|^{\frac{1}{p}} < 1/2.$$

The estimates (12), (13), (14) and (17) yield that $\mathcal{T}_1 + \mathcal{T}_2$ maps $B_\varepsilon(0)$ into itself and is a contraction on this ball. Hence, the Banach fixed point argument completes the proof of the existence of a solution to equation (10) in $B_\varepsilon(0)$. \square

3.4. Main existence theorem. Combining the geometric assumptions on the \tilde{u} -nullcline with the regularity and perturbation lemmas, we now establish the existence of far-from-equilibrium stationary solutions. The result is obtained by applying the localised branch-switching lemma to the (\tilde{v}, \tilde{w}) -subsystem and reconstructing \tilde{u} from the chosen nullcline branch.

Theorem 3.5. *Consider problem (5) with a constant solution \bar{X} satisfying Assumption 3.1 and Assumption 3.2. There exists $\delta > 0$ such that for any open subset $\Omega_1 \subseteq \Omega$ with $\Omega_2 = \Omega \setminus \bar{\Omega}_1$ satisfying $|\Omega_2| < \delta$, problem (5) admits a weak solution $(\tilde{v}, \tilde{w}) = (\tilde{v}(x), \tilde{w}(x))$ to*

$$D_v \Delta \tilde{v} + g(\tilde{u}, \tilde{v}, \tilde{w}) = 0 \quad \text{and} \quad D_w \Delta \tilde{w} + h(\tilde{v}, \tilde{w}, \tilde{u}) = 0,$$

where

$$(18) \quad \tilde{u}(x) = \begin{cases} \varphi(\tilde{v}(x), \tilde{w}(x)), & x \in \Omega_1, \\ \psi(\tilde{v}(x), \tilde{w}(x)), & x \in \Omega_2, \end{cases}$$

satisfies $f(\tilde{u}(x), \tilde{v}(x), \tilde{w}(x)) = 0$ for almost all $x \in \bar{\Omega}$.

Proof. Let us choose $\varepsilon > 0$ so small that $B(\bar{v}, \bar{w}, \varepsilon) \subseteq \mathcal{V} \times \mathcal{W}$. First, we restrict φ and ψ to $B(\bar{v}, \bar{w}, \varepsilon)$ and then we extend them in arbitrary way to $\tilde{\varphi}, \tilde{\psi} \in C_b^2(\mathbb{R}^{m_d}, \mathbb{R}^{m_u})$ such that $\tilde{\varphi} = \varphi$ on $B(\bar{v}, \bar{w}, \varepsilon)$ and analog for $\tilde{\psi}$. Now, we define

$$(19) \quad q_1(v, w) = \begin{pmatrix} g(\tilde{\varphi}(v, w), v, w) \\ h(\tilde{\varphi}(v, w), v, w) \end{pmatrix} \quad \text{and} \quad q_2(v, w) = \begin{pmatrix} g(\tilde{\psi}(v, w), v, w) \\ h(\tilde{\psi}(v, w), v, w) \end{pmatrix},$$

which satisfy assumptions of Lemma 3.4. Obviously $q_1, q_2 \in C^2(\mathbb{R}^{m_d}, \mathbb{R}^{m_d})$ together with $q_1(\bar{v}, \bar{w}) = 0$. Using $f(\varphi(v, w), v, w) = 0$ on $B_\varepsilon(0)$, one can calculate

$$(20) \quad \nabla_{(v,w)} \tilde{\varphi}(\bar{v}, \bar{w}) = \begin{pmatrix} -\nabla_u f(\bar{X})^{-1} \nabla_v f(\bar{X}) \\ -\nabla_u f(\bar{X})^{-1} \nabla_w f(\bar{X}) \end{pmatrix}.$$

The same holds for $\nabla_{(v,w)} \tilde{\psi}(\bar{v}, \bar{w})$. For notational simplicity, we write $\nabla f := \nabla f(\bar{X})$ and use similar abbreviations for other derivatives.

Then, using Assumption 3.1, (19), (20) and applying Schur's formula for determinants of block matrices, we obtain

$$\det(\nabla_{(v,w)}q_1(\tilde{v},\tilde{w}) - D^d\lambda_j) = \frac{1}{\det(\nabla_u f)} \det(J - D\lambda_j) \neq 0.$$

Hence for each $p \in [2, \infty)$, by Lemma 3.4, we obtain a solution $(\tilde{v}, \tilde{w}) \in W_\nu^{2,p}(\Omega)^{m_d}$ to problem (9) which satisfy $\|\tilde{v} - \bar{v}\|_{W^{2,p}} + \|\tilde{w} - \bar{w}\|_{W^{2,p}} \leq \varepsilon$ for arbitrary small $\varepsilon > 0$ provided $|\Omega_2| > 0$ is sufficiently small. By the Sobolev embedding $L^\infty(\Omega) \subseteq W^{2,p}(\Omega)$ with $p > N/2$ and $\varepsilon > 0$ small enough, we obtain $\tilde{\varphi} = \varphi$ and $\tilde{\psi} = \psi$ for all $x \in \Omega$ which completes the construction of solution to problem (5). \square

Remark 3.6 (Proximity to \bar{X}). *The stationary solution $(\tilde{u}, \tilde{v}, \tilde{w})$ constructed in Theorem 3.5 stays close to the points $(\bar{u}, \bar{v}, \bar{w})$ and $(\psi(\bar{v}, \bar{w}), \bar{v}, \bar{w})$ in the following sense. There exists $\varepsilon_0 > 0$ such that, for every $\varepsilon \in (0, \varepsilon_0)$, we find $\delta(\varepsilon) > 0$ such that the solution constructed in Theorem 3.5 satisfies*

$$(21) \quad \begin{aligned} \|\tilde{v} - \bar{v}\|_{L^\infty} &< \varepsilon, & \|\tilde{w} - \bar{w}\|_{L^\infty} &< \varepsilon, \quad \text{and} \\ \|\tilde{u} - \varphi(\bar{u})\|_{L^\infty(\Omega_1)} + \|\tilde{u} - \psi(\bar{u})\|_{L^\infty(\Omega_2)} &< C\varepsilon. \end{aligned}$$

If such solution is stable, we refer to it as far-from-equilibrium patterns since the solution is "far away" from the equilibrium $(\bar{u}, \bar{v}, \bar{w})$ on Ω_2 (depending on the distance of the two branches of $f = 0$).

Remark 3.7 (Continuity and jumps). *By Sobolev embedding, the diffusive components \tilde{v} and \tilde{w} belong to $C(\bar{\Omega})$ and are therefore continuous. In contrast, the nondiffusive component \tilde{u} , defined by (18), may exhibit jump discontinuities across $\partial\Omega_1$ whenever $\varphi(\nu, \omega) \neq \psi(\nu, \omega)$ in $\mathcal{V} \times \mathcal{W}$. Such discontinuities occur when the parameter $\varepsilon > 0$ in (21) is chosen sufficiently small.*

Remark 3.8 (Multiplicity). *The subset $\Omega_2 \subset \Omega$ can be chosen arbitrarily, provided its measure is sufficiently small, yielding infinitely many distinct stationary solutions. Stability of these patterns is a separate issue, potentially influenced by the geometry of Ω_2 and the values of the diffusion coefficients. In practice, Ω_2 does not need to be very small, as illustrated in Section 6.*

4. GENERAL CONDITIONS FOR DIFFUSION-DRIVEN INSTABILITY

In this section we derive sufficient conditions for diffusion-driven instability (DDI), the classical mechanism underlying Turing patterns. As recalled in Section 2, a spatially homogeneous steady state \bar{X} exhibits DDI if it is stable to homogeneous perturbations but destabilized by heterogeneous ones for suitable diffusion coefficients. In this case, stationary periodic structures – the classical close-to-equilibrium Turing patterns – may emerge. Unlike the far-from-equilibrium patterns studied in the previous section, here the relative magnitudes of the diffusion coefficients D_v and D_w play a decisive role.

Let \bar{X} denote a constant steady state of system (1), and let $J = \nabla_{(u,v,w)}F(\bar{X})$ denote the Jacobian at \bar{X} . Since we focus on DDI, we assume throughout that J is stable. Also recall the notation from (4).

4.1. When DDI cannot occur. By (2) and (3), DDI is excluded if

- (i) J_1 is stable,
- (ii) $J - D$ is stable for all diagonal matrices $D \geq 0$

Matrices satisfying condition (ii) are called *strongly stable*. For 2×2 or 3×3 matrices, strong stability is equivalent to the stability of J and all its principal submatrices [3, Theorems 3–4]. For higher dimensions this equivalence fails: stability of all principal submatrices does not

guarantee strong stability[23, Example 3.1]. In that case ($m > 3$), DDI is possible even if every lower-dimensional subsystem is stable.

Theorem 4.1 (Volterra-Lyapunov stability). *If there exists a diagonal matrix $M > 0$ such that $JM + MJ^T$ is negative definite matrix, then the constant steady state \bar{X} is stable for all diffusion coefficients D_v, D_w .*

Proof. The matrix J satisfying $JM + MJ^T < 0$ for some diagonal matrix $M > 0$ is strongly stable and all submatrices of J are semistable [3, Proposition 1, Theorem 1]. By (2) and (3), we have $s(\mathcal{L}) \leq 0$ for all diffusion coefficients D_v, D_w . \square

4.2. Autocatalysis of non-diffusing components. Instability of a principal submatrix immediately precludes strong stability. The most prominent case is subsystem J_1 , associated with the nondiffusive variables. If $s(J_1) > 0$ while $s(J) < 0$, then diffusion always induces instability. This is referred to as the *autocatalysis condition*.

Theorem 4.2. *Suppose $s(J) < 0$ and $s(J_1) > 0$. Then the steady state \bar{X} exhibits DDI for all diffusion matrices $D_v, D_w > 0$. Moreover, every Turing pattern in a neighborhood of \bar{X} is unstable.*

Proof. Since $s(J) < 0$ while (2) yields $s(\mathcal{L}) \geq s(J_1) > 0$ for all $D_v, D_w > 0$, the steady state \bar{X} is stable with respect to spatially homogeneous perturbations but unstable with respect to heterogeneous ones.

To show that all Turing patterns are unstable, let $\tilde{X} = (\tilde{u}, \tilde{v}, \tilde{w})$ be a continuous, nonconstant stationary solution of (1) intersecting \bar{X} . Choose $x_0 \in \Omega$ such that $\tilde{X}(x_0) = \bar{X}$ and let $\tilde{\mathcal{L}}$ denote the linearization at \tilde{X} . By (2), the assumption $s(J_1) > 0$, the spectral characterization of $\nabla_u f(\tilde{X})$ from [5, Lemma 4.4], and the continuity of \tilde{X} , we have

$$s(\tilde{\mathcal{L}}) \geq s(\nabla_u f(\tilde{X})) > 0,$$

which completes the proof. \square

This autocatalysis condition was already identified in the classical Turing framework. The additional conclusion – that nearby Turing patterns are unstable – highlights the sharp destabilizing effect of an unstable nondiffusive block.

To find conditions for DDI under which Turing patterns are possible, we are interested in a different mechanism.

4.3. Instability induced by non- and slow-diffusing components. Diffusion-driven instability can also originate in the coupled block J_{12} governing both m_u nondiffusive and m_v slow-diffusive variables, without requiring instability of J_1 . Writing the linearized operator \mathcal{L} explicitly depending on the diffusion coefficients as \mathcal{L}_{D_v, D_w} , we obtain:

Theorem 4.3. *If $s(\mathcal{L}_{0, \hat{D}}) > 0$ for some fast diffusion matrix $\hat{D} > 0$, then there exists $\varepsilon > 0$ such that $s(\mathcal{L}_{D_v, \hat{D}}) > 0$ for all slow diffusion matrices $0 \leq D_v < \varepsilon$.*

Proof. Consider fixed diffusion coefficients $\hat{D} > 0$ such that $s(\mathcal{L}_{0, \hat{D}}) > 0$. First, we show that this implies the existence of an eigenvalue of $\mathcal{L}_{0, \hat{D}}$ with strictly positive real part. If such an eigenvalue exists directly, we proceed with the continuity argument. Otherwise, by (2), any spectral element λ with $\operatorname{Re} \lambda > 0$ belongs to $\sigma(J_{12})$. Then, by [13, Section 2.1.2], there exists a sequence of eigenvalues $\mu_j \in \sigma(J - \lambda_j D)$ such that $\mu_j \rightarrow \lambda$ as $j \rightarrow \infty$, with $\operatorname{Re} \mu_j > 0$ for sufficiently large j .

Next, we use the continuity of eigenvalues with respect to diffusion parameters. The point spectrum of \mathcal{L}_{D_v, D_w} is characterized by roots of the characteristic polynomial

$$P(\lambda; \lambda_j, D_v, D_w) = \det(\lambda I + \lambda_j D - J),$$

see (3). Since polynomial roots depend continuously on their coefficients [4], eigenvalues vary continuously with D_v and D_w . Because there exists $k \in \mathbb{N}_0$ such that $P(\lambda; \lambda_k, 0, \hat{D})$ has a root with positive real part, we can choose $\varepsilon > 0$ small enough so that for all $0 \leq D_v < \varepsilon$, $P(\lambda; \lambda_j, D_v, \hat{D})$ retains a root with positive real part. \square

Remark 4.4. *Combining the results of Theorem 4.3 and (3), we conclude that*

$$s(\mathcal{L}) > 0 \iff \exists j \in \mathbb{N}_0 : s(-\lambda_j D + J) > 0.$$

New sufficient conditions for DDI follow directly from Theorem 4.3.

Corollary 4.5. *If the Jacobian matrix J is stable while the principal submatrix J_{12} is unstable, then the constant steady state \bar{X} exhibits DDI for any fixed $D_w > 0$ and sufficiently small $D_v \geq 0$.*

Remark 4.6. *The conditions for DDI do not require the presence of all three component types: nondiffusive, slow-diffusive, and fast-diffusive in the model (1). For Theorem 4.2, it suffices to have at least one nondiffusive component and at least one diffusive component, i.e., $m_u \geq 1$ and $m_v + m_w \geq 1$. Corollary 4.5 applies also to classical reaction-diffusion systems, where all components diffuse. In that case, minimal assumptions are $m_v \geq 1$ and $m_w \geq 1$.*

4.4. Large fast diffusion and domain rescaling. Rather than considering small slow diffusion rates D_v , we may alternatively examine the effect of large fast diffusion coefficients D_w . A rescaling argument yields:

Corollary 4.7. *Let $D_v > 0$ be fixed and suppose $s(\mathcal{L}_{0, \hat{D}}) > 0$ for some $\hat{D} > 0$. Then, there exists $d_0 \geq 1$ and $L_0 \geq 1$ such that*

$$s(\mathcal{L}_{D_v, d\hat{D}}) > 0 \quad \text{for all } d \geq d_0$$

when $\mathcal{L}_{D_v, d\hat{D}}$ is considered on the scaled domain $L\Omega$ with $L \geq L_0$.

Proof. The claim follows by rescaling the system, applying Theorem 4.3, and then transforming back to the original variables. Since Theorem 4.3 is stated for a fixed domain, the rescaling may result in a larger spatial domain $L\Omega$ with $L \geq 1$.

Assume $s(\mathcal{L}_{0, \hat{D}}) > 0$ for some $\hat{D} > 0$ and fix $D_v = \text{diag}(d_1, \dots, d_{m_v})$. By Theorem 4.3, there exists $\varepsilon > 0$ such that

$$s(\mathcal{L}_{D_v, \hat{D}}) > 0 \quad \text{for all } 0 \leq D < \varepsilon.$$

Choose $\tilde{d} \geq 1$ so that $d_i/\tilde{d} < \varepsilon$ for every $i = 1, \dots, m_v$. Then $s(\mathcal{L}_{\frac{1}{\tilde{d}}D_v, \hat{D}}) > 0$ for all $d \geq \tilde{d}$.

Rescaling space by the factor \sqrt{d} transforms the domain to

$$\tilde{\Omega} = \sqrt{d}\Omega =: L_d\Omega$$

and gives $s(\mathcal{L}_{D_v, d\hat{D}}) > 0$ for all $d \geq \tilde{d}$. Since $\tilde{d} \geq 1$, we have $L_d \geq 1$, with $L_{\tilde{d}} = 1$ if $\varepsilon > 0$ is large enough to ensure $d_i < \varepsilon$ for all i . \square

Remark 4.8. *Increasing only D_w while keeping D_v fixed is, in general, insufficient to induce DDI. An enlargement of the spatial domain with fixed D_v is required, since this effectively decreases D_v relative to D_w and thereby restores the instability mechanism. Example 5.3 illustrates a case where enlarging the domain is essential for the occurrence of DDI.*

4.5. Instabilities beyond J_1 and J_{12} . While our main results highlight J_1 and J_{12} as natural candidates for driving diffusion–driven instability, destabilization can also arise from other subsystems. In particular, interactions within the block J_{23} , coupling slow and fast diffusers, may generate instability under suitable diffusion rates (Example 5.2). Moreover, in certain cases instability does not correspond to any single identifiable subsystem, but rather emerges from the collective interplay of all components [23, Example 3.1]. These scenarios indicate that, although J_1 and J_{12} provide transparent mechanisms for diffusion–driven instability, the broader landscape of destabilization phenomena in reaction–diffusion–ODE systems is richer and cannot always be reduced to low-dimensional subsystems only. To illustrate this point concretely, we systematically analyze in Section 5 all possible sources of diffusion–driven instability in the minimal setting of a three-component system consisting of one nondiffusive, one slow-diffusive, and one fast-diffusive variable.

5. GENERAL SYSTEM CONSISTING OF 1 ODE AND 2 PDEs

In this section, we examine whether diffusion–driven instability (DDI) can arise from subsystems beyond those previously considered – specifically, subsystems other than J_1 and J_{12} . While identifying pattern-forming reaction–diffusion systems that exhibit DDI remains challenging, it is well known that coupling stable reaction–diffusion subsystems with nondiffusive components can destabilize the constant steady state. Our previous results show that this occurs when the nondiffusive component is itself unstable or forms an unstable subsystem together with some diffusive components.

Here, we highlight a subtler mechanism: a stable two-component diffusive system can become unstable through the addition of a stable nondiffusive component, even when this component does not belong to any unstable subsystem. The coupling alone may destabilize the diffusive subsystem, thereby generating DDI and enabling pattern formation.

To analyze this systematically, we consider a reaction–diffusion–ODE system (1) with one nondiffusive and two diffusive components, setting $m_u = m_v = m_w = 1$ with $D_v > 0$ and $D_w > 0$. We fix a constant steady state $\bar{X} = (\bar{u}, \bar{v}, \bar{w}) \in \mathbb{R}^3$ and denote the linearization around \bar{X} by \mathcal{L} . The 3×3 Jacobian matrix at \bar{X} and its subsystems are defined in (4).

We first summarize the results from the previous section. The constant steady state \bar{X} exhibits DDI if $s(J) < 0$ and one of the following conditions holds:

- | | | |
|-------------------------|---------------------------|---------------------------|
| (22) (i) $J_1 > 0$, | D_v arbitrary, | D_w arbitrary, |
| (ii) $s(J_{12}) > 0$, | D_v sufficiently small, | D_w fixed, |
| (iii) $s(J_{13}) > 0$, | D_v fixed, | D_w sufficiently small. |

To fully characterize DDI in case of three equations, we also mention the case of J_{13} unstable which does not necessarily fit to our setting with v slow-diffusive and w fast-diffusive but rather is the mirrored situation switching components v and w .

For a three-equation system, the conditions for DDI can be made explicit via the Routh–Hurwitz criterion. Following [2], let

$$P(\lambda) = \lambda^3 + p_1\lambda^2 + p_2\lambda + p_3$$

be the characteristic polynomial of J , with

$$p_1 = -\text{tr } J, \quad p_2 = \det J_{12} + \det J_{23} + \det J_{13}, \quad p_3 = -\det J.$$

The Routh–Hurwitz criterion establishes that J is stable (i.e., all roots of $P(\lambda)$ lie in the left half-plane) if and only if

$$p_1 > 0, \quad p_3 > 0, \quad p_1 p_2 - p_3 > 0,$$

which also ensure $p_2 > 0$. We assume $s(J) < 0$, a necessary condition for DDI.

DDI requires \bar{X} to be unstable under spatially heterogeneous perturbations, i.e., $s(\mathcal{L}) > 0$. By Remark 4.4, this is equivalent to the existence of $j \in \mathbb{N}_0$ such that $s(-\lambda_j D + J) > 0$, where λ_j denotes j -th eigenvalue of Laplacian $-\Delta$. We consider the characteristic polynomial of $-\mu D + J$ for $\mu \geq 0$:

$$P(\lambda; \mu) = \det(\lambda I + \mu D - J) = \lambda^3 + p_1(\mu)\lambda^2 + p_2(\mu)\lambda + p_3(\mu),$$

with coefficients

$$\begin{aligned} p_1(\mu) &= \text{tr}(\mu D - J), \\ p_2(\mu) &= \det(J_{12} - \mu D_{12}) + \det(J_{23} - \mu D_{23}) + \det(J_{13} - \mu D_{13}), \\ p_3(\mu) &= \det(\mu D - J). \end{aligned}$$

Since J is stable, it holds $p_1(\mu) > 0$ for all $\mu \geq 0$. By the Routh–Hurwitz criterion, instability of \mathcal{L} occurs if either

$$p_3(\mu) < 0 \quad \text{or} \quad p_1(\mu)p_2(\mu) - p_3(\mu) < 0$$

for some $\mu = \lambda_j$. In this case, \bar{X} exhibits DDI.

We now identify which subsystems of J must be unstable in order for the steady state \bar{X} to exhibit DDI.

Proposition 5.1. *If \bar{X} exhibits DDI, then J is stable and at least one of the subsystems J_1 , J_{12} , J_{13} , or J_{23} is unstable.*

Proof. By [2, Theorem 1.2], if J and all its 1- and 2-component subsystems are stable, the steady state is stable for all D_v, D_w , contradicting DDI. Direct calculation confirms that $p_3(\mu) > 0$ and $p_1(\mu)p_2(\mu) - p_3(\mu) > 0$ for all $\mu \geq 0$ when $J_1, J_{12}, J_{13}, J_{23}$, and J are all stable. Hence, $J_2 > 0$ or $J_3 > 0$ alone cannot induce DDI. \square

The cases J_1 and J_{12} (and J_{13}) are already covered by (22). The case $s(J_{23}) > 0$ is treated next, showing that it can destabilize \bar{X} in certain situations, though it is not sufficient for DDI in general.

5.1. Instability induced by the diffusive components. We now focus on J_{23} , the subsystem of slow- and fast-diffusive components. The interest in the case $s(J_{23}) > 0$ stems from the observation that, after applying a quasi-steady-state reduction to the nondiffusive variable, the resulting purely diffusive system is often regarded as determining the onset of DDI. However, even if this reduced system is stable and shows no DDI on its own, coupling it back to the nondiffusive component may destabilize the full system. In particular, an unstable J_{23} can sometimes trigger DDI, though this is not guaranteed.

For instance, [2, Theorem 1.1] ensures DDI from $s(J_{23}) > 0$ when the diffusion rates of v and w are sufficiently smaller than of u . In our case, u is nondiffusive, so this result does not directly apply, motivating a detailed Routh–Hurwitz analysis. If J_{12} and J_{23} are stable, then

$$p_3(\mu) = p_3 + [(\det J_{13})D_v + (\det J_{12})D_w]\mu - J_1 D_v D_w \mu^2 > 0$$

for all $\mu \geq 0$. Moreover,

$$\begin{aligned} p_1(\mu)p_2(\mu) - p_3(\mu) &= p_1p_2 - p_3 \\ &+ [(\det J_{12} + \det J_{23} + \text{tr } J \text{tr } J_{13})D_v + (\det J_{23} + \det J_{13} + \text{tr } J \text{tr } J_{12})D_w]\mu \\ &+ [-\text{tr } J_{13}D_v^2 - \text{tr } J_{12}D_w^2 - 2\text{tr } JD_vD_w]\mu^2 + (D_v^2D_w + D_vD_w^2)\mu^3. \end{aligned}$$

Here, the condition $\det J_{23} < 0$ is crucial for obtaining $p_1(\mu)p_2(\mu) - p_3(\mu) < 0$ for some $\mu \geq 0$, while $p_2 = \det J_{12} + \det J_{23} + \det J_{13}$ must remain positive and sufficiently large to ensure $p_1p_2 - p_3 > 0$, thereby guaranteeing $s(J) < 0$.

Example 5.2. *We choose*

$$J = \begin{pmatrix} -1 & 9 & 1.5 \\ -9 & -1 & 5 \\ -2 & 3.5 & -1 \end{pmatrix}.$$

A direct computation yields

$$s(J) < 0, \quad J_1 < 0, \quad J_2 < 0, \quad J_3 < 0, \quad s(J_{12}) < 0, \quad s(J_{13}) < 0, \quad s(J_{23}) > 0$$

and

$$\begin{aligned} p_1(\mu)p_2(\mu) - p_3(\mu) &= 3.75 + (-6.5D_w + 71.5D_v)\mu \\ &+ (2D_v^2 + 2D_w^2 + 6D_vD_w)\mu^2 + (D_v^2D_w + D_vD_w^2)\mu^3. \end{aligned}$$

For instance, choosing $D_v = 0.001$ and $D_w = 1$ gives

$$p_1(\mu)p_2(\mu) - p_3(\mu) < 0 \text{ for } \mu \in (0.767, 2.433).$$

On $\Omega = (0, \pi)$ with $\lambda_1 = 1 \in (0.767, 2.433)$, we obtain $s(\mathcal{L}) > 0$, so the system exhibits DDI.

Interestingly, reducing the system to the two diffusive components, the steady state is stable and no DDI occurs. Indeed, consider the linear system

$$\partial_t \begin{pmatrix} u \\ v \\ w \end{pmatrix} = \begin{pmatrix} 0 \\ D_v \Delta v \\ D_w \Delta w \end{pmatrix} + \begin{pmatrix} -1 & 9 & 1.5 \\ -9 & -1 & 5 \\ -2 & 3.5 & -1 \end{pmatrix} \begin{pmatrix} u \\ v \\ w \end{pmatrix}.$$

Applying the quasi-steady-state approximation (QSSA) to eliminate u yields the reduced Jacobian

$$\bar{J} = \begin{pmatrix} -82 & -8.5 \\ -14.5 & -4 \end{pmatrix}, \quad \text{tr } \bar{J} = -86 < 0, \quad \det \bar{J} = 204.75 > 0.$$

Since \bar{J} and its principal submatrices are stable, the reduced system is stable for all choice of diffusions $D_v, D_w > 0$.

5.2. Increasing the domain for large diffusion. As noted in Remark 4.8, increasing the spatial domain is generally necessary to obtain DDI when the slow-diffusive coefficient D_v is fixed and smaller than the fast-diffusive coefficient D_w . Scaling the domain without rescaling variables increases all nonzero diffusion coefficients. Since D_v remains unchanged in such a scaling, the ratio D_v/D_w effectively decreases, which can move the system into a DDI regime. The following example illustrates this effect and clarifies when and how domain changes influence instability.

Example 5.3. Consider the linear operator

$$\mathcal{L}_d = D\Delta + J, \quad D = \begin{pmatrix} 0 & & \\ & 1 & \\ & & d \end{pmatrix}, \quad J = \begin{pmatrix} -1 & 1 & -3 \\ 2 & -1 & -5 \\ 2 & 1 & -1.5 \end{pmatrix},$$

with $d > 0$ on the domain $\Omega = (0, 1)$. A direct computation gives $s(J) < 0$ and $s(J_{12}) > 0$, so by (22) system exhibits DDI if d and the domain Ω are sufficiently large.

Without rescaling Ω , $p_1(\mu)p_2(\mu) - p_3(\mu) > 0$ for all $d > 0$ and $\mu \geq 0$, and $p_3(\mu) > 0$ whenever $\mu \notin (0, 1)$. For any $\varepsilon \in (0, 1/2)$, choosing $d > 116.5$ sufficiently large, we have $p_3(\mu) < 0$ for $\mu \in (\varepsilon, 1 - \varepsilon)$. On $\Omega = (0, 1)$, the Laplacian eigenvalues satisfy $\lambda_0 = 0$ and $\lambda_j > 1$ for all $j \geq 2$. Hence, $s(\mathcal{L}_d) < 0$ for all $d > 0$. However, scaling the domain to $\tilde{\Omega} = L\Omega$ with $L \geq 1$ large enough yields $\lambda_1 \in (\varepsilon, 1 - \varepsilon)$ and $s(\mathcal{L}_d) > 0$.

Remark 5.4. Using the Routh–Hurwitz criterion, one can explicitly determine the domain scaling required for DDI with unstable J_{12} assuming $s(J) < 0$, $J_1 < 0$, D_v fixed and D_w arbitrarily large. Depending on whether $\text{tr } J_{12} > 0$, $\det J_{12} < 0$, or both, one can estimate the leading-order terms of p_3 and $p_1p_2 - p_3$ in D_w to determine the range of μ where instability of $-\mu D + J$ occurs, and thus choose L such that λ_1 lies within this range. From this, we obtain:

- Case $\text{tr } J_{12} > 0$:

For $\varepsilon \in (0, \frac{\text{tr } J_{12}}{2D_s})$, there exists $D_w > 0$ sufficiently large such that

$$p_1(\mu)p_2(\mu) - p_3(\mu) < 0 \quad \text{for } \mu \in \left(\varepsilon, \frac{\text{tr } J_{12}}{D_v} - \varepsilon\right).$$

Choosing $L \geq 1$ large enough so that $\lambda_1 < \text{tr } J_{12}/D_v$ for the first positive Laplacian eigenvalue λ_1 on $L\Omega$ yields DDI.

- Case $\det J_{12} < 0$:

For $\varepsilon \in (0, \frac{\det J_{12}}{2J_1 D_s})$, there exists $D_w > 0$ sufficiently large such that

$$p_3(\mu) < 0 \quad \text{for } \mu \in \left(\varepsilon, \frac{\det J_{12}}{J_1 D_s} - \varepsilon\right).$$

Choosing $L \geq 1$ so that $\lambda_1 < \det J_{12}/(J_1 D_s)$ yields DDI for large D_f .

- Case $\text{tr } J_{12} > 0$ and $\det J_{12} < 0$: DDI occurs for large D_w if

$$\lambda_1 \in \left(0, \max \left\{ \frac{\text{tr } J_{12}}{D_s}, \frac{\det J_{12}}{J_1 D_s} \right\}\right).$$

6. APPLICATION TO A SIMPLIFIED RECEPTOR-BASED MODEL

In this section, we illustrate the theoretical framework developed above by applying it to a receptor-based model consisting of one ODE and two PDEs. The model is inspired by [19], and describes the dynamics of receptors (u), ligands (v), and enzymes (w) on a one-dimensional spatial domain.

Let $\Omega = (0, L) \subset \mathbb{R}$, with $L > 0$. The governing equations are

$$(23) \quad \begin{cases} \partial_t u = -\mu_1 u + m_1 uv(1 + uv)^{-1}, & \text{for } x \in \bar{\Omega}, t > 0, \\ \partial_t v = D_v \Delta v - \mu_2 v + m_2 uv(1 + uv)^{-1} - vw, & \text{for } x \in \Omega, t > 0, \\ \partial_t w = D_w \Delta w - \mu_3 w + m_3 uv(1 + uv)^{-1}, & \text{for } x \in \Omega, t > 0, \end{cases}$$

supplemented with homogeneous Neumann boundary conditions for v and w , and nonnegative initial data. Here $\mu_i \in (0, 1]$ denote decay rates, $m_i \in [2, +\infty)$ are production rates, $D_v, D_w > 0$

are diffusion coefficients, and the receptor population u is assumed immobile. The nonlinear production terms follow a Michaelis–Menten type saturation in the ligand–receptor binding.

Introducing $X = (u, v, w)^T$, $X_0 = (u_0, v_0, w_0)^T$, and $D = \text{diag}(0, D_v, D_w)$, the system takes the vector form as

$$\partial_t X = D\Delta X + F(X), \quad \text{for } x \in \Omega \text{ and } t > 0,$$

with nonlinearities

$$F(X) = \begin{pmatrix} -\mu_1 u + m_1 uv(1+uv)^{-1} \\ -\mu_2 v + m_2 uv(1+uv)^{-1} - vw \\ -\mu_3 w + m_3 uv(1+uv)^{-1} \end{pmatrix} = \begin{pmatrix} f(X) \\ g(X) \\ h(X) \end{pmatrix}.$$

Existence, uniqueness, and boundedness of solutions are established in Appendix B.

For the analysis of DDI, we require that the reduced kinetic system

$$\dot{X}(t) = F(X(t)), \quad X(0) = X_0,$$

possesses a positive, asymptotically stable steady state. To simplify the notation, we introduce the quantities

$$(24) \quad \eta_1 := \frac{m_1}{\mu_1}, \quad \eta_2 := \frac{m_2}{\mu_2}, \quad \eta_3 := \frac{m_3}{\mu_3}, \quad \alpha := m_2\eta_1 - \eta_3.$$

To formulate the upcoming results, we first collect the parameter constraints into the following assumption.

Assumption 6.1. *Let $\mu_i \in (0, 1]$, $m_i \geq 2$ for $i = 1, 2, 3$, and $\eta_1, \eta_2, \eta_3, \alpha$ be as in (24). We assume:*

- (1) $\zeta > 0$, where $\zeta := \alpha - 2\mu_2$,
- (2) $\Theta > 0$, where $\Theta := \zeta^2 - 4\mu_2(\mu_2 + \eta_3)$,
- (3) $\alpha + 2\eta_3 + \sqrt{\Theta} > 2\left(\frac{\mu_1}{\mu_3} - 1\right)(\mu_2 + \eta_3)\frac{\eta_1\eta_3}{m_1 + m_2}$.

Under Assumption 6.1, the kinetic system admits three nonnegative steady states, as stated below.

Theorem 6.2. *Under Assumption 6.1 the associated kinetic system admits three constant steady states:*

$$\bar{X}_0 := (0, 0, 0) \quad \text{and} \quad \bar{X}_\pm := (\bar{u}_\pm, \bar{v}_\pm, \bar{w}_\pm),$$

with

$$\bar{v}_\pm = \frac{\alpha + 2\eta_3 \pm \sqrt{\Theta}}{2\eta_1(\mu_2 + \eta_3)}, \quad \bar{u}_\pm = \eta_1 - \frac{1}{\bar{v}_\pm}, \quad \bar{w}_\pm = \eta_3 - \frac{\eta_3}{\eta_1 \bar{v}_\pm}.$$

Here, \bar{X}_0 is stable, \bar{X}_- is positive and unstable, and \bar{X}_+ is positive and asymptotically stable.

The proof of this result is given in Appendix A. Assume from now on that the conditions of Theorem 6.2 hold.

6.1. Diffusion-driven instability. We now investigate whether the stable positive steady state \bar{X}_+ can destabilize through diffusion-driven instability. Since \bar{X}_0 is Volterra–Lyapunov stable (Theorem 4.1) and \bar{X}_- is unconditionally unstable, only \bar{X}_+ is relevant for DDI.

Let $J := J(\bar{X}_+)$ be the Jacobian matrix of the nonlinearities F evaluated at \bar{X}_+ . A transformation using the relation $F(\bar{X}_+) = 0$, allows us to express J as follows:

$$J = \frac{1}{(1 + \bar{u}_+ \bar{v}_+)^2} \begin{pmatrix} -m_1 \bar{u}_+ \bar{v}_+^2 & m_1 \bar{u}_+ & 0 \\ m_2 \bar{v}_+ & -m_2 \bar{u}_+^2 \bar{v}_+ & -\bar{v}_+ (1 + \bar{u}_+ \bar{v}_+)^2 \\ m_3 \bar{v}_+ & m_3 \bar{u}_+ & -\mu_3 (1 + \bar{u}_+ \bar{v}_+)^2 \end{pmatrix}.$$

The diagonal element $J_1 < 0$ rules out the autocatalysis condition of Theorem 4.2. Furthermore, the 2×2 submatrices J_{13} and J_{23} are stable (negative trace, positive determinant), leaving J_{12} as the only viable source of DDI (Corollary 4.5, Proposition 5.1).

Theorem 6.3 (Instability of J_{12}). *Suppose Assumption 6.1 holds and, in addition,*

$$(4) \quad \eta_1 < 2 \left(\frac{\eta_3}{m_2} + \frac{2}{\eta_2} \right).$$

Then J_{12} has an unstable eigenvalue. Consequently, there exists either $D_v > 0$ sufficiently small, or a pair (D_w, L) with $D_w > 0$ and $L \geq 1$ both sufficiently large, such that \bar{X}_+ undergoes DDI.

Proof. From $\text{tr}(J_{12}) = -\bar{u}_+ \bar{v}_+ (m_1 \bar{v}_+ + m_2 \bar{u}_+)$, it is clear that the sub-matrix J_{12} has a negative trace. Thus, the 2×2 matrix J_{12} has an eigenvalue with positive real part if and only if $\det J_{12} < 0$. This occurs when the parameters satisfy

$$\det(J_{12}) = m_1 m_2 \frac{\bar{u}_+ \bar{v}_+}{(1 + \bar{u}_+ \bar{v}_+)^4} ((\bar{u}_+ \bar{v}_+)^2 - 1) < 0.$$

Clearly, this inequality holds whenever $\bar{u}_+ \bar{v}_+ < 1$. By definition of \bar{u}_+ , the inequality is satisfied when $\bar{v}_+ < 2/\eta_1$. Substituting the explicit expression for \bar{v}_+ , we obtain

$$(25) \quad \alpha + \sqrt{\alpha^2 - 4\mu_2(\alpha + \eta_3)} < 2(\eta_3 + 2\mu_2).$$

Using the definition of α , inequality (25) simplifies to the desired condition $\eta_1 < 2(\frac{\eta_3}{m_2} + \frac{2}{\eta_2})$.

If this inequality is satisfied, then $s(J_{12}) > 0$. By Corollaries 4.5 and 4.7, there exists either $D_v > 0$ sufficiently small, or a pair (D_w, L) with $D_w > 0$ and $L \geq 1$ both sufficiently large, such that the steady state \bar{X}_+ exhibits DDI. \square

Theorem 6.3 guarantees the existence of DDI under broad parameter regimes. The threshold values of D_v , D_w , and L in Theorem 6.3 can be characterized explicitly using the Routh–Hurwitz criterion applied to the characteristic polynomial of $J - \lambda_j D$ (Theorem 6.4). See Section 5 for the notation. For this system, it is straightforward to verify that the Routh–Hurwitz elements $p_1(\lambda_j)$, $p_2(\lambda_j)$, and $(p_1 p_2 - p_3)(\lambda_j)$ are positive for all $\lambda_j \geq 0$ and $D_v, D_w > 0$. Instability can therefore arise only if D_v and D_w are chosen such that, for some fixed eigenvalue λ_j the Routh–Hurwitz element $p_3(\lambda_j) := -\det(J - \lambda_j D)$ is negative.

Theorem 6.4. *Let $\Omega = (0, L)$ and consider the constant steady state \bar{X}_+ of (23). This steady state exhibits DDI if either of the following conditions is satisfied:*

(I) $L > 0$, the diffusion coefficient $D_w > 0$ is fixed and

$$0 < D_v < \varepsilon := \sup_{j \in \mathbb{N}} \frac{\det(J) - \det(J_{12}) D_w \lambda_j}{\lambda_j (\det(J_{13}) - J_1 D_w \lambda_j)},$$

(II) $D_v > 0$ fixed, and

$$L > \pi j \sqrt{\frac{J_1 D_v}{\det(J_{12})}}, \quad D_w > \frac{\det(J) - \det(J_{13}) D_v \lambda_j}{\lambda_j (\det(J_{12}) - J_1 D_v \lambda_j)} > 0$$

holds for at least one $j \in \mathbb{N}$.

Proof. To determine the precise parameter regimes for DDI, we analyze the sign of the Routh–Hurwitz element $p_3(\lambda_j) = -\det(J - \lambda_j D)$. Instability requires $p_3(\lambda_j) < 0$, and we distinguish the cases of small D_v and large D_w accordingly.

By solving $p_3(\lambda_j) < 0$ for D_v , that is, finding values of D_v such that

$$-\det(J) + \left(\det(J_{13}) D_v + \det(J_{12}) D_w \right) \lambda_j + \left(-J_1 D_v D_w \right) \lambda_j^2 < 0,$$

we obtain condition (I). The right-hand side of the resulting inequality is positive for sufficiently large $j \in \mathbb{N}$ and converges to 0, since J_{12} is unstable while J_1 and J_{13} are always stable.

The second condition is obtained by fixing $j \in \mathbb{N}$ and rewriting $p_3(\lambda_j) < 0$ as

$$(26) \quad \lambda_j (\det(J_{12}) - J_1 D_v \lambda_j) D_w < \det(J) - \det(J_{13}) D_v \lambda_j.$$

Since the right-hand side of (26) is negative, this inequality can only hold for large D_w if

$$\det(J_{12}) - J_1 D_v \lambda_j < 0.$$

The latter can always be achieved by increasing the domain length L if necessary. Solving (26) for D_w and the above inequality for L yields the two expressions stated in condition (II). \square

6.2. Numerical simulation. We first verify that the parameter constraints introduced in Assumption 6.1 and Theorem 6.3 define a non-empty region. These conditions guarantee the existence of the asymptotically stable steady state \bar{X}_+ and the occurrence of diffusion-driven instability through $s(J_{12}) > 0$.

Let $p := (m_1, m_2, m_3, \mu_1, \mu_2, \mu_3)$ denote the vector collecting parameters of system (23), and $\mathcal{P} := [2, +\infty)^3 \times [0, 1]^3$ the admissible parameter domain. Within \mathcal{P} we define

$$\begin{aligned} \mathcal{R}_1 &:= \left\{ p \in \Pi : \zeta > 0, \text{ where } \zeta := \alpha - 2\mu_2 \right\}, \\ \mathcal{R}_2 &:= \left\{ p \in \Pi : \Theta > 0, \text{ where } \Theta := \zeta^2 - 4\mu_2(\mu_2 + \eta_3) \right\}, \\ \mathcal{R}_3 &:= \left\{ p \in \Pi : \alpha + 2\eta_3 + \sqrt{\Theta} > 2 \left(\frac{\mu_1}{\mu_3} - 1 \right) (\mu_2 + \eta_3) \frac{\eta_1 \eta_3}{m_1 + m_2} \right\}, \\ \mathcal{R}_4 &:= \left\{ p \in \Pi : \eta_1 < 2 \left(\frac{\eta_3}{m_2} + \frac{2}{\eta_2} \right) \right\}, \end{aligned}$$

A numerical exploration shows that

$$p_* = (2.5, 9.68, 7.0, 0.95, 0.95, 0.6) \in \bigcap_{i=1}^4 \mathcal{R}_i,$$

confirming that the feasible region is non-empty. Since the inequalities defining $\mathcal{R}_1, \dots, \mathcal{R}_4$ are strict, an open neighborhood $\mathcal{V}_{p_*} \subset \mathcal{P}$ exists in which all constraints remain satisfied (see Figure 1).

The bifurcation structure of system (23) can be characterized using the Routh–Hurwitz polynomial p_3 , whose roots determine stability boundaries in the diffusion parameter plane. The Turing-unstable region consists of all pairs of diffusion coefficients for which at least one spatial mode becomes unstable. For each spatial eigenmode λ_j , define

$$\Gamma_j := \left\{ (D_v, D_w) \in (\mathbb{R}_{>0})^2 : p_3(\lambda_j; D_v, D_w) < 0 \right\}, \quad j \in \mathbb{N},$$

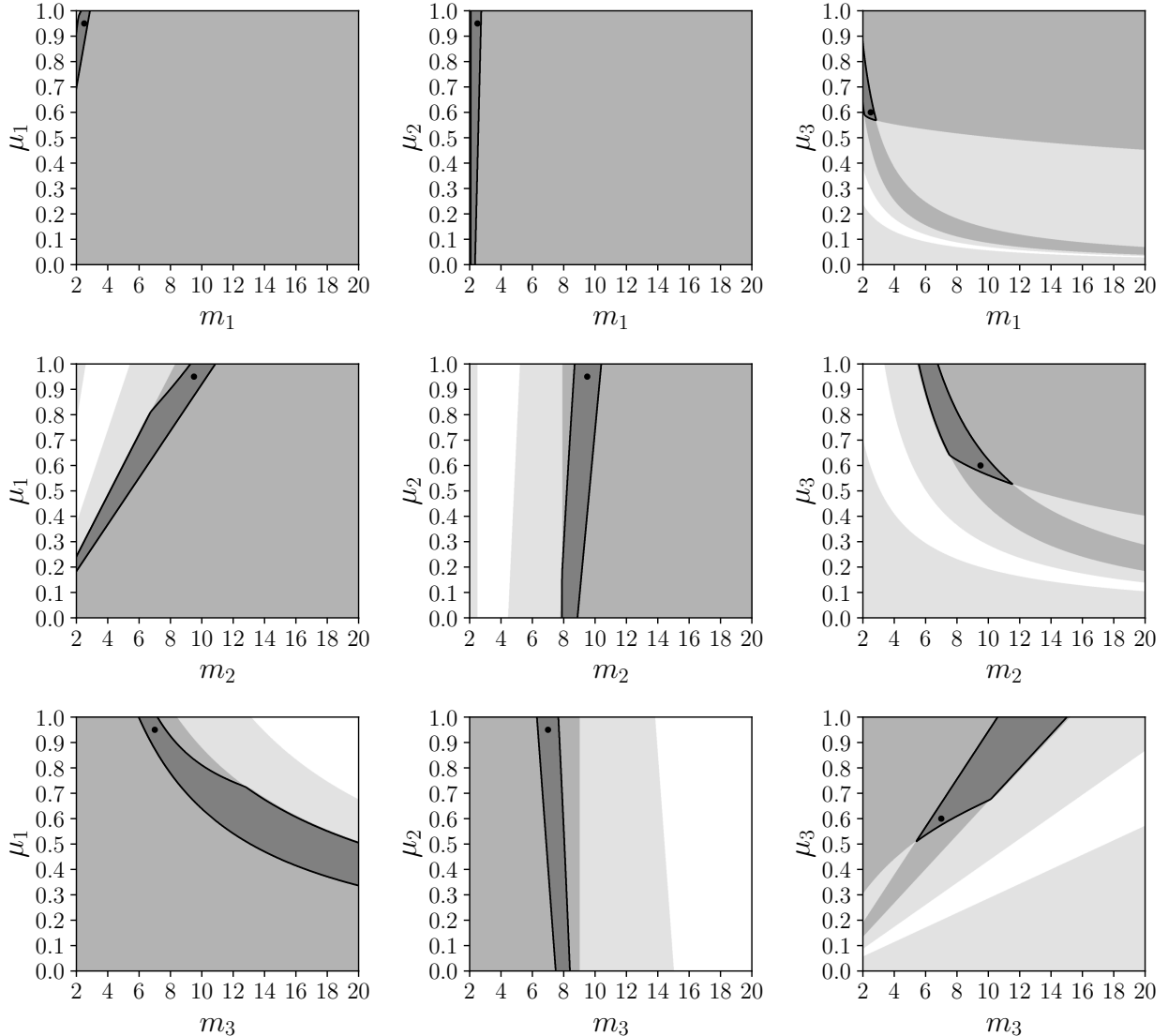


FIGURE 1. Cross sections of the six-dimensional parameter space, \mathcal{R} , in the (m_i, μ_j) -planes, $i, j = 1, 2, 3$. In each panel, the regions $\mathcal{R}_1, \dots, \mathcal{R}_4$ are superimposed. The overlap, enclosed by a black curve, corresponds to parameters satisfying all constraints simultaneously. The black dot marks the feasible point p_\star .

where the dependence of p_3 on D_v and D_w is made explicit. Here, $\partial\Gamma_j$ denotes the associated stability curve $p_3(\lambda_j; D_v, D_w) = 0$. Each Γ_j consists of diffusion pairs destabilizing the j -th mode. If $(D_v, D_w) \in \Gamma_{i_1} \cap \dots \cap \Gamma_{i_k}$, the linearized operator at \bar{X}_+ has at least k unstable eigenvalues. The full Turing-unstable set is therefore

$$\Gamma := \bigcup_{j=1}^{\infty} \Gamma_j.$$

Any diffusion pair $(D_v, D_w) \in \Gamma$ induces DDI of the steady state \bar{X}_+ . Figure 2 illustrates the structure of Γ and its constituent regions. This description permits selective pattern control: choosing (D_v, D_w) within a prescribed Γ_j excites the j -th spatial mode, so that, with suitable

initial conditions, patterns with a predictable number of peaks can be generated. Representative simulations on $\Omega = (0, 1)$ are shown in Figure 3.

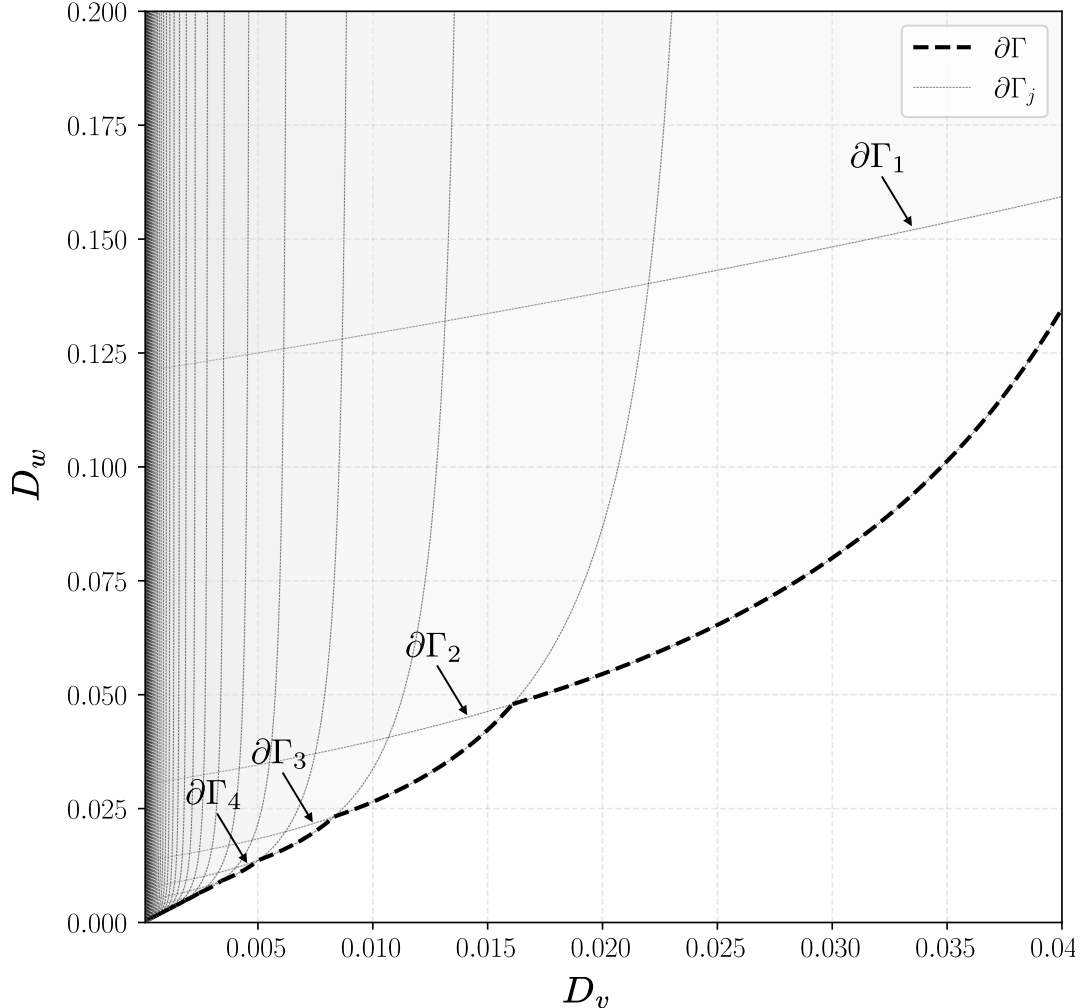


FIGURE 2. Bifurcation diagram for system (23) in the (D_v, D_w) -plane. The shaded region Γ is the Turing unstable set, given by the union of all mode-specific regions Γ_j .

Parameters: $\mu_1 = 1.00, \mu_2 = 1.00, \mu_3 = 0.60, m_1 = 2.50, m_2 = 9.68, m_3 = 7.00$.

6.3. Turing pattern vs. far-from-equilibrium patterns. We distinguish between two fundamentally different types of spatial patterns. First, there are *Turing patterns*, which are defined as regular structures that bifurcate from a constant steady state through diffusion-driven instability. Their spatial scale is dictated by the unstable eigenmodes of the linearized operator. In contrast, we observe *Far-from-equilibrium patterns*, which do not rely on DDI: they may exist as isolated solution branches, exhibit discontinuities or spikes, and form a continuum of stationary states depending on the nonlinear reaction terms. These patterns do not exist in classical reaction–diffusion systems, but are intrinsic to mixed ODE–PDE dynamics. Importantly, distinguishing between these pattern types can be challenging, as both types of patterns can evolve from a perturbation of a constant steady state exhibiting DDI.

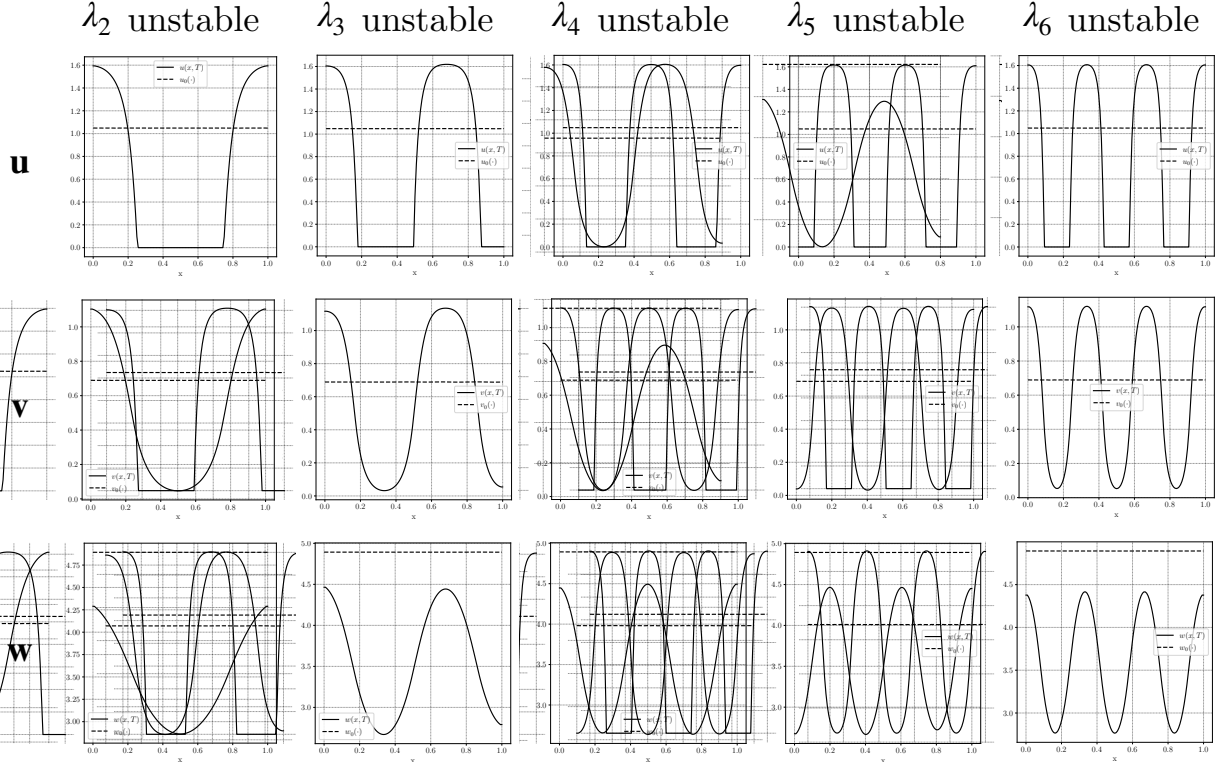


FIGURE 3. Patterned solutions to system (23). Each row corresponds to one component of $X = (u, v, w)$; each column shows the outcome for a different diffusion pair (D_v, D_w) . In all cases, only a single spatial mode is unstable.

Parameters: $\mu_1 = 1.00, \mu_2 = 1.00, \mu_3 = 0.60, m_1 = 2.50, m_2 = 9.68, m_3 = 7.00$.

Init. Cond.: $u_0 = \bar{u} + \xi, \quad v_0 = \bar{v} + \xi, \quad w_0 = \bar{w} + \xi, \quad \xi = \frac{x}{10} \sin(10\pi x)$.

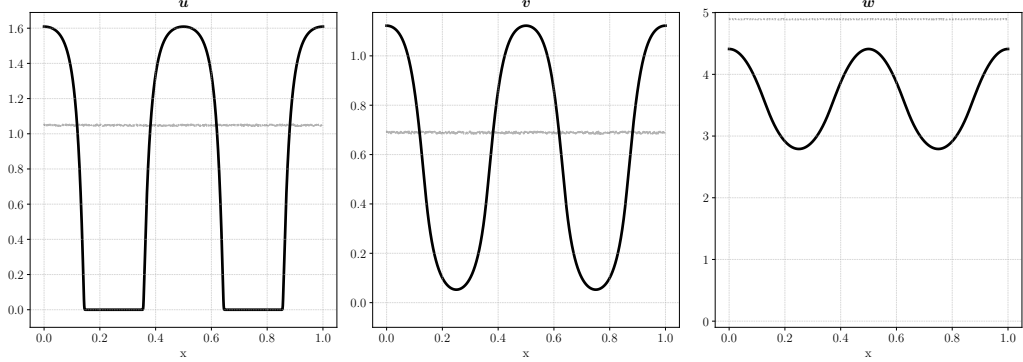
The patterns observed in our simulations of system (23) highlight the connection between classical Turing instability and far-from-equilibrium dynamics. To understand their nature, recall the nullcline for the nondiffusive component, $\{(u, v) \in \mathbb{R}^2 : f(u, v) = 0\}$, consists of two branches:

$$u = 0 \quad \text{and} \quad u = \frac{m_1}{\mu_1} - \frac{1}{v},$$

and the constant steady state \bar{X}_+ exhibiting DDI lies on the nontrivial branch. When perturbed by small random noise, the emerging patterns are initially governed by the unstable eigenmodes of the Laplacian: if only the j -th eigenmode is unstable, the spatial structure behaves similarly to $\cos(j\pi x/L)$ with the corresponding number of peaks, see Fig. 3.

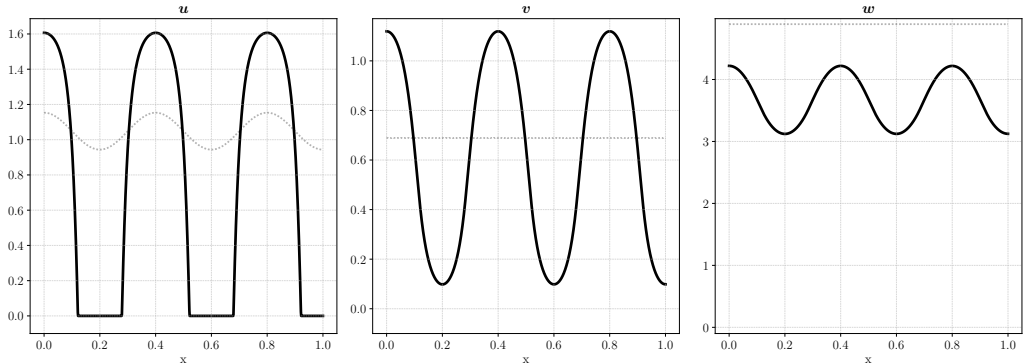
Surprisingly, nonlinear interactions allow stable patterns associated with higher modes that are *linearly stable*. Intuitively, Figure 4 shows that, when λ_4 is the only unstable mode, large-amplitude perturbations aligned with $\cos(5\pi x)$ or $\cos(6\pi x)$ in the nondiffusive component still yield patterns reflecting those modes. This demonstrates that nonlinearity can stabilize patterns which otherwise would be beyond the reach of classical Turing instability, provided the perturbation is strong enough to escape the basin of attraction of the unstable eigenmode.

A main observation that distinguishes patterns presented in Figure 3 and Figure 4 from classical Turing patterns is that rather than stabilizing near the constant steady state, solutions



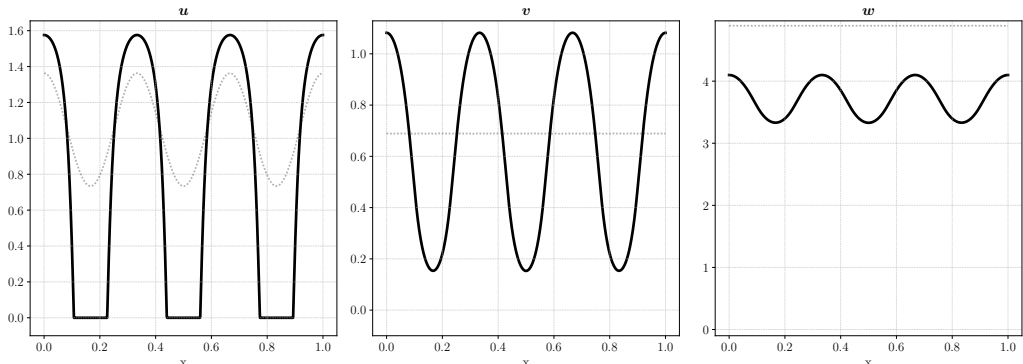
(A) Small random perturbation around \bar{X} :

Init. Cond.: $u_0 = \bar{u} + \xi$, $v_0 = \bar{v} + \xi$, $w_0 = \bar{w} + \xi$, $\xi = 0.01 \cdot \mathcal{U}(-1, 1)$



(B) Perturbation describing eigenmode λ_5 :

Init. Cond.: $u_0 = \bar{u} + 0.1 \cdot \bar{u} \cos(5\pi x)$, $v_0 = \bar{v} + \xi$, $w_0 = \bar{w} + \xi$, $\xi = 0.01 \cdot \mathcal{U}(-1, 1)$



(C) Perturbation describing eigenmode λ_6 :

Init. Cond.: $u_0 = \bar{u} + 0.1 \cdot \bar{u} \cos(6\pi x)$, $v_0 = \bar{v} + \xi$, $w_0 = \bar{w} + \xi$, $\xi = 0.01 \cdot \mathcal{U}(-1, 1)$

FIGURE 4. Patterns from simulations with $D_v = 0.006$ and $D_w = 0.017$, for which only the eigenmode λ_4 is unstable. Different initial conditions select patterns associated with different eigenmodes.

Parameters: $\mu_1 = 1.00$, $\mu_2 = 1.00$, $\mu_3 = 0.60$, $m_1 = 2.50$, $m_2 = 9.68$, $m_3 = 7.00$.

drift toward the trivial branch $u \equiv 0$ of the nullcline, where they settle into stable far-from-equilibrium patterns. This branch-switching mechanism explains both the non-smooth structure of the u state variable in Fig. 3 (despite their Turing-like appearance), and the discontinuous stationary states constructed in Fig. 5. Thus, while unstable eigenmodes originating from

DDI act as a selection mechanism, the observed patterns are ultimately far-from-equilibrium states determined by the structure of the nonlinear branch. We recreate this property by varying initial conditions, see Figure 4 for comparison.

Theorem 3.5 provides the theoretical foundation: for any sufficiently small subset $\Omega_2 \subset \Omega$, one can construct stationary solutions in which u switches between the two nullcline branches. These patterns do not require DDI for their existence, only the presence of multiple solution branches satisfying Assumptions 3.1–3.2. This yields uncountably many distinct far-from-equilibrium patterns, in stark contrast to the discrete set of Turing modes in classical reaction-diffusion systems. The continuum of possibilities arises because Ω_2 may be chosen arbitrarily, producing a rich family of spatial organizations not captured by bifurcation from a steady state. In fact, it is possible to construct patterns that are arbitrarily close in the L^2 -norm. Consequently, none of these patterns can be *asymptotically* stable in L^2 , since for every such pattern one can find an arbitrarily close initial condition that is itself a stationary solution. In contrast, the same patterns are not close in the L^∞ -norm, which allows for the possibility of asymptotic stability in L^∞ .

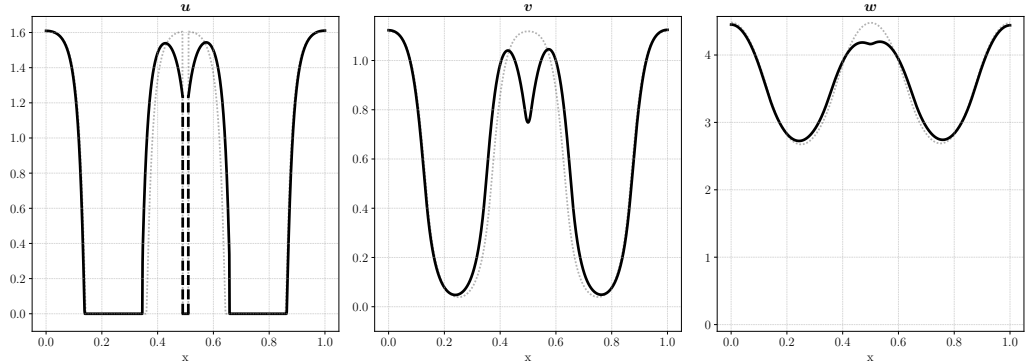
Figure 5 illustrates this mechanism explicitly. Starting from a continuous pattern obtained near DDI, we force u to jump to the trivial branch on small subsets of the domain. The resulting stationary profiles exhibit genuine jump discontinuities in u , yet remain stable under time evolution. This shows that discontinuous patterns are not artifacts of numerics but inherent to the system’s dynamics.

In the case of stable Turing patterns, one would expect that choosing diffusion coefficients closer to the threshold for DDI would yield patterns of smaller amplitude, as the system is near to the bifurcation point. In such a regime, the patterns should arise purely on the nontrivial branch of the nullcline $f = 0$ not using any far-from-equilibrium dynamics. However, this behavior is never observed in our simulations.

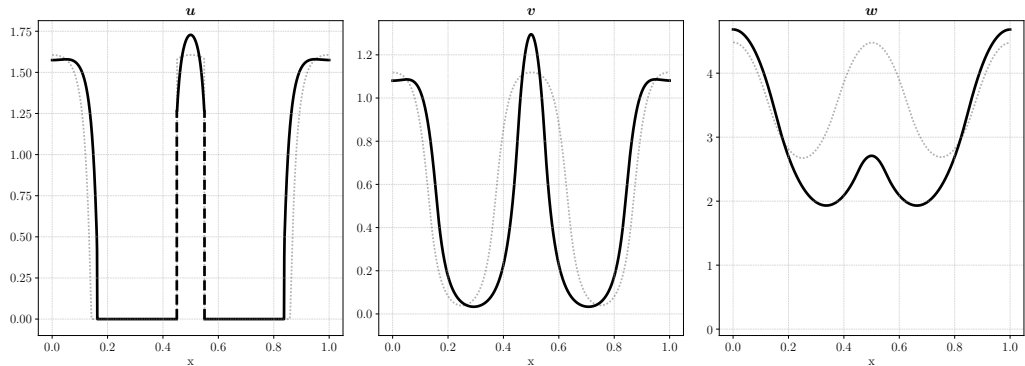
In conclusion, although the patterns in system (23) may resemble classical Turing patterns, their origin is fundamentally different: unstable eigenmodes associated with DDI act only as a catalyst, guiding the solution toward far-from-equilibrium states created by branch switching in the nondiffusive component. This hybrid mechanism enriches the pattern formation landscape and highlights phenomena that cannot occur in standard reaction-diffusion systems.

ACKNOWLEDGMENT

This work is supported by the German Research Foundation (DFG) under Germany’s Excellence Strategy EXC 2181/1 - 390900948 (the Heidelberg STRUCTURES Excellence Cluster) and through the Collaborative Research Center 1324 (SFB1324, project B6).



(A) Initial profile forced to zero on $(0.49, 0.51)$ produces two jump discontinuities at $x = 0.49$ and $x = 0.51$ (dashed black).



(B) Forcing $u = 0$ on two subintervals $(0.35, 0.45)$ and $(0.55, 0.65)$ produces jumps at $x = 0.45$ and $x = 0.55$ (dashed black).

FIGURE 5. Simulation of System (23) with initial condition (dotted gray) taken from the pattern in Figure 3 (λ_4 unstable) and modified by introducing an artificial jump to zero as indicated in the subfigures. The resulting stationary profile (black) exhibits jump discontinuities.

Parameters: $\mu_1 = 1.00$, $\mu_2 = 1.00$, $\mu_3 = 0.60$, $m_1 = 2.50$, $m_2 = 9.68$, $m_3 = 7.00$.

REFERENCES

- [1] G. Akagi, I. Takagi, and C. Zhang. Steady states with jump discontinuity in a receptor-based model with hysteresis in higher-dimensional domains. *SIAM Journal on Mathematical Analysis*, 56(2):1996–2033, 2024.
- [2] A. Anma, K. Sakamoto, and T. Yoneda. Unstable subsystems cause turing instability. *Kodai Mathematical Journal*, 35(2):215–247, 2012.
- [3] G. W. Cross. Three types of matrix stability. *Linear Algebra and its Applications*, 20:253–263, 1978.
- [4] F. Cucker and A. Corbalan. An alternate proof of the continuity of the roots of a polynomial. *The American Mathematical Monthly*, 96(4):342–345, 1989.
- [5] S. Cygan, A. Marciniak-Czochra, G. Karch, and K. Suzuki. Instability of all regular stationary solutions to reaction-diffusion-ODE systems. *Journal of Differential Equations*, 337:460–482, 2022.
- [6] S. Cygan, A. Marciniak-Czochra, G. Karch, and K. Suzuki. Stable discontinuous stationary solutions to reaction-diffusion-ODE systems. *Communications in Partial Differential Equations*, 47(10):2023–2053, 2022.

- Equations*, 48(3):478–510, 2023.
- [7] M. Daub. An Appropriate Bounded Invariant Region for a Bistable Reaction-Diffusion Model of the Caspase-3/8 Feedback Loop. *Bulletin of Mathematical Biology*, 75(11):2271–2288, Nov. 2013.
- [8] P. Grisvard. *Elliptic Problems in Nonsmooth Domains*. Pitman Publishing, 1985.
- [9] G. Guo, X. Yang, C. Zhang, and S. Li. Pattern formation with jump discontinuity in a predator-prey model with Holling-II functional response. *European Journal of Applied Mathematics*, page 1–23, 2025.
- [10] X. He, K. Y. Lam, Y. Lou, and W. M. Ni. Dynamics of a consumer-resource reaction-diffusion model. *Journal of Mathematical Biology*, 78:1605–1636, 2019.
- [11] S. Härtig, A. Marciniak-Czochra, and I. Takagi. Stable patterns with jump discontinuity in systems with turing instability and hysteresis. *Discrete and Continuous Dynamical Systems*, 37:757–800, 2017.
- [12] A. Iuorio, M. B. Eppinga, M. Baudena, F. Veerman, M. Rietkerk, and F. Giannino. Modelling how negative plant-soil feedbacks across life stages affect the spatial patterning of trees. *Scientific Reports*, 13(1):19128, 2023.
- [13] V. Klika, R. Baker, D. Headon, and E. Gaffney. The influence of receptor-mediated interactions on reaction-diffusion mechanisms of cellular self-organisation. *Bulletin of Mathematical Biology*, 74(4):935—957, 2012.
- [14] A. Köthe, A. Marciniak-Czochra, and I. Takagi. Hysteresis-driven pattern formation in reaction-diffusion-ODE systems. *Discrete and Continuous Dynamical Systems*, 40:3595–3627, 2020.
- [15] C. Kowall. *Uniform shadow limit reduction for reaction-diffusion-ODE systems*. PhD thesis, Heidelberg University, 2021.
- [16] C. Kowall, A. Marciniak-Czochra, and F. Münnich. Nonlinear stability results for stationary solutions of reaction-diffusion-ODE systems. *Journal of Differential Equations*, 448:113704, 2025.
- [17] A. Lunardi. *Analytic semigroups and optimal regularity in parabolic problems*. Springer Science & Business Media, 2012.
- [18] A. Marasco, A. Iuorio, F. Cartení, G. Bonanomi, D. M. Tartakovsky, S. Mazzoleni, and F. Giannino. Vegetation pattern formation due to interactions between water availability and toxicity in plant-soil feedback. *Bulletin of Mathematical Biology*, 76:2866–2883, 2014.
- [19] A. Marciniak-Czochra. Receptor-based models with hysteresis for pattern formation in hydra. *Mathematical Biosciences*, 199:97–119, 2006.
- [20] A. Marciniak-Czochra. Strong two-scale convergence and corrector result for a receptor-based model of intercellular communication. *IMA Journal of Applied Mathematics*, 77(6):855–868, 2012.
- [21] A. Marciniak-Czochra, M. Nakayama, and I. Takagi. Pattern formation in a diffusion-ODE model with hysteresis. *Differential and Integral Equations*, 28:655–694, 2015.
- [22] A. Marciniak-Czochra and M. Ptashnyk. Derivation of a macroscopic receptor-based model using homogenization techniques. *SIAM Journal on Mathematical Analysis*, 40(1):215–237, 2008.
- [23] R. A. Satnoianu and P. van den Driessche. Some remarks on matrix stability with application to turing instability. *Linear Algebra and its Applications*, 398:69–74, 2005.
- [24] J. Smoller. *Shock waves and reaction-diffusion equations*. Springer New York, 1983.
- [25] I. Takagi and C. Zhang. Pattern formation in a reaction-diffusion-ODE model with hysteresis in spatially heterogeneous environments. *Journal of Differential Equations*, 280:928–966, 2021.

- [26] C. Zhang, L. Hou, and Y. Lu. Dynamic behaviors of a receptor-based model. *International Journal of Biomathematics*, 2025.

APPENDIX A. PROOF OF THEOREM 6.2

We now prove Theorem 6.2. The argument is divided into three steps. First, we show that the system admits three steady states when condition 2 holds. Second, we establish that the two nontrivial steady states are positive under condition 1. Finally, we analyze the Jacobian to determine that \bar{X}_+ is locally asymptotically stable, while \bar{X}_- is unstable, under condition 3.

Proof. Step I: Analysis of steady states. It is clear $\bar{X}_0 := 0$ is a constant steady state. At equilibrium, the relation $\frac{\partial \bar{u}}{\partial t} = 0$ implies $\bar{u} = \eta_1 - \frac{1}{\bar{v}}$, and substituting the expression of \bar{u} into $\frac{\partial \bar{w}}{\partial t} = 0$ gives $\bar{w} = \eta_3(1 - \frac{1}{\eta_1 \bar{v}})$. Plugging both relations into $\frac{\partial \bar{v}}{\partial t} = 0$ yields a quadratic equation that \bar{v} must obey:

$$(27) \quad \eta_1(\mu_2 + \eta_3)\bar{v}^2 - (\alpha + 2\eta_3)\bar{v} + m_2 = 0.$$

The discriminant

$$(28) \quad (\alpha + 2\eta_3)^2 - 4m_2\eta_1(\mu_2 + \eta_3) = (\alpha - 2\mu_2)^2 - 4\mu_2(\mu_2 + \eta_3)$$

is positive thanks to assumption 2. Thus, equation (27) has two distinct real solutions and overall, system (23) admits three constant steady states: the trivial equilibrium \bar{X}_0 , and two nontrivial steady states $\bar{X}_\pm = (\eta_1 - \frac{1}{\bar{v}_\pm}, \bar{v}_\pm, \eta_3 - \frac{\eta_3}{\eta_1 \bar{v}_\pm})$, where

$$\bar{v}_\pm := \frac{\alpha + 2\eta_3 \pm \sqrt{(\alpha - 2\mu_2)^2 - 4\mu_2(\mu_2 + \eta_3)}}{2\eta_1(\mu_2 + \eta_3)}.$$

Step II: Positivity of the nontrivial steady states. It is straightforward to verify $\bar{v}_\pm > 0$ for all admissible parameters. From $\bar{u}_\pm = \eta_1 - 1/\bar{v}_\pm$ and $\bar{w}_\pm = \eta_3(1 - 1/(\eta_1 \bar{v}_\pm))$, both \bar{u}_\pm , and \bar{w}_\pm are positive, if $\eta_1 \bar{v}_\pm > 1$. Substituting the expression for \bar{v}_\pm gives the inequality

$$(29) \quad \mp \sqrt{(\alpha - 2\mu_2)^2 - 4\mu_2(\mu_2 + \eta_3)} < \alpha - 2\mu_2.$$

Recall that condition 1 ensures $\alpha - 2\mu_2 > 0$. In the “-” case, inequality (29) holds automatically since the left-hand side is negative and the right-hand side is positive. In the “+” case, both sides of equation (29) are positive, and the inequality (29) holds again. Therefore, both \bar{X}_\pm are positive.

Step III: Stability analysis. We investigate conditions under which the system is bistable. The Jacobian evaluated at an arbitrary equilibrium $\bar{X} = (\bar{u}, \bar{v}, \bar{w})$ is

$$J(\bar{X}) = \frac{1}{(1 + \bar{u}\bar{v})^2} \begin{pmatrix} -\mu_1(1 + \bar{u}\bar{v})^2 + m_1\bar{v} & m_1\bar{u} & 0 \\ m_2\bar{v} & -(\mu_1 + \bar{w})(1 + \bar{u}\bar{v})^2 + m_2\bar{u} & -\bar{v}(1 + \bar{u}\bar{v})^2 \\ m_3\bar{v} & m_3\bar{u} & -\mu_3(1 + \bar{u}\bar{v})^2 \end{pmatrix}.$$

First, we observe $J(\bar{X}_0) = -\text{diag}(\mu_1, \mu_2, \mu_3)$, which is clearly stable. However, more work is needed to conclude about the stability of J around \bar{X}_\pm . Exploiting relations on the steady-states, we obtain

$$J(\bar{X}_\pm) = \frac{1}{(1 + \bar{u}_\pm \bar{v}_\pm)^2} \begin{pmatrix} -m_1\bar{u}_\pm \bar{v}_\pm^2 & m_1\bar{u}_\pm & 0 \\ m_2\bar{v}_\pm & -m_2\bar{u}_\pm^2 \bar{v}_\pm & -\bar{v}_\pm(1 + \bar{u}_\pm \bar{v}_\pm)^2 \\ m_3\bar{v}_\pm & m_3\bar{u}_\pm & -\mu_3(1 + \bar{u}_\pm \bar{v}_\pm)^2 \end{pmatrix}.$$

Our next step is to use the Routh-Hurwitz criterion to show that J is unstable around \bar{X}_- , and stable around \bar{X}_+ .

Computing $\det(J(\bar{X}_\pm))$ yields

$$\begin{aligned}\det(J(\bar{X}_\pm)) = & \frac{1}{(1 + \bar{u}_\pm \bar{v}_\pm)^6} \left[\bar{v}_\pm (1 + \bar{u}_\pm \bar{v}_\pm)^2 \left(-m_1 m_3 \bar{u}_\pm^2 \bar{v}_\pm^2 - m_1 m_3 \bar{u}_\pm \bar{v}_\pm \right) \right. \\ & \left. - \mu_3 (1 + \bar{u}_\pm \bar{v}_\pm)^2 \left(m_1 m_2 \bar{u}_\pm^3 \bar{v}_\pm^3 - m_1 m_2 \bar{u}_\pm \bar{v}_\pm \right) \right].\end{aligned}$$

Using the definition of \bar{u}_\pm , we establish $\bar{u}_\pm \bar{v}_\pm - 1 = \eta_1 \bar{v}_\pm - 2$. Thus,

$$(30) \quad \det(J(\bar{X}_\pm)) = -m_1 \mu_3 \frac{\bar{u}_\pm \bar{v}_\pm}{(1 + \bar{u}_\pm \bar{v}_\pm)^3} \left[(\alpha + 2\eta_3) \bar{v}_\pm - 2m_2 \right].$$

For convenience, we introduce the notation

$$\beta := \alpha + 2\eta_3 > 0, \quad \gamma := 4\mu_2(\alpha + \eta_3) > 0, \quad \delta := 4\eta_3(\alpha + \eta_3) > 0.$$

Substituting the expression of \bar{v}_\pm into (30) yields

$$-\det(J(\bar{X}_\pm)) = m_1 \mu_3 \frac{\bar{u}_- \bar{v}_-}{(1 + \bar{u}_- \bar{v}_-)^3} \left(\frac{\beta}{2\eta_1(\mu_2 + \eta_3)} (\beta \pm \sqrt{\alpha^2 - \gamma}) - 2m_2 \right).$$

We stress that the square roots have positive argument, since $\alpha^2 - \gamma > 0$ by assumption 2. Factoring the $2\eta_1(\mu_2 + \eta_3)$ term out, we obtain

$$-\det(J(\bar{X}_\pm)) = \frac{\mu_1 \mu_3}{2(\mu_2 + \eta_3)} \frac{\bar{u}_- \bar{v}_-}{(1 + \bar{u}_- \bar{v}_-)^3} \left(\beta^2 - \delta - \gamma \pm \beta \sqrt{\alpha^2 - \gamma} \right).$$

Using $\beta^2 - \delta = \alpha^2$, we see that $-\det(J(\bar{X}_\pm))$ has the same sign as

$$\mathcal{A} := \alpha^2 - \gamma \pm \beta \sqrt{\alpha^2 - \gamma} = \sqrt{\alpha^2 - \gamma} \left(\sqrt{\alpha^2 - \gamma} \pm \beta \right).$$

We deal with the case "−" and "+" separately. In the "−" case, it holds

$$\mathcal{A} = \frac{\sqrt{\alpha^2 - \gamma}}{\sqrt{\alpha^2 - \gamma} + \beta} (\alpha^2 - \beta^2 - \gamma) = -\frac{\sqrt{\alpha^2 - \gamma}}{\sqrt{\alpha^2 - \gamma} + \beta} (\delta + \gamma) < 0,$$

so $-\det(J(\bar{X}_-)) < 0$ and the Routh-Hurwitz criterion enables us to conclude that \bar{X}_- is unstable. On the other hand, in the "+" case, $\mathcal{A} > 0$ follows from (28). Thus $-\det(J(\bar{X}_+)) > 0$. Using the Routh-Hurwitz criterion once again, the steady state \bar{X}_+ is stable if

$$(31) \quad -\text{tr}(J(\bar{X}_+)) \left(\sum_{1 \leq i < j \leq 3} \det(J(\bar{X}_+)_{ij}) \right) + \det(J(\bar{X}_+)) > 0.$$

This last expression is rather involved, so we break it down into smaller parts. Using the positivity of all terms in $-\text{tr}(J(\bar{X}_+))$, we obtain the (coarse) estimate $-\text{tr}(J(\bar{X}_+)) > \mu_3$. Next, by distributing $\frac{m_1}{(1 + \bar{u}_+ \bar{v}_+)^2}$ inside the parenthesis in equation (30), the coefficient $-\det(J(\bar{X}_+))$ is rewritten as

$$-\det(J(\bar{X}_+)) = \mu_3 \frac{u_+ v_+}{(1 + \bar{u}_+ \bar{v}_+)^2} \left(\frac{m_1 \eta_3 \bar{v}_+}{1 + \bar{u}_+ \bar{v}_+} - m_1 m_2 \frac{1 - \bar{u}_+ \bar{v}_+}{1 + \bar{u}_+ \bar{v}_+} \right).$$

Finally, a direct computation shows

$$\sum_{1 \leq i < j \leq 3} \det(J(\bar{X}_+)_{ij}) = \mu_3 \frac{u_+ v_+}{(1 + \bar{u}_+ \bar{v}_+)^2} \left(m_1 \bar{v}_+ + m_2 \bar{u}_+ + \eta_3 - \frac{m_1 m_2}{\mu_3} \frac{1 - \bar{u}_+ \bar{v}_+}{1 + \bar{u}_+ \bar{v}_+} \right).$$

Putting everything together, inequality (31) holds if

$$m_1\bar{v}_+ + m_2\bar{u}_+ + \eta_3 > \frac{m_1\eta_3}{(1 + \bar{u}_+\bar{v}_+)\mu_3}\bar{v}_+.$$

Using the equality $1 + \bar{u}_+\bar{v}_+ = \eta_1\bar{v}_+$ with the estimate $\bar{u}_+ > \bar{v}_+$, we rewrite the last inequality as

$$\bar{v}_+ > \left(\frac{\mu_1}{\mu_3} - 1\right) \frac{\eta_3}{m_1 + m_2}.$$

This inequality holds thanks to assumption 3. Hence, \bar{X}_+ is locally asymptotically stable. Therefore, the kinetic system is bistable under our assumptions and the proof is completed. \square

APPENDIX B. EXISTENCE OF A NONNEGATIVE, BOUNDED, GLOBAL SOLUTION TO SYSTEM (23)

In this section, we show that the system (23) has a global solution, which is nonnegative and bounded, using a bounded invariant region argument. Kowall et al. [16, Proposition C.2] recently established that RD-ODE systems of the form (23) admit a unique local-in-time mild solution. We denote such a solution by $X = (u, v, w)$.

Our goal here is to extend this local solution to all times, by proving that solutions to (23) remain *a priori* bounded for all time. This is achieved using the theory of bounded invariant regions (see [24, Chap. 14, §B]). We first recall the definition of an invariant region.

Definition B.1 (Invariant Region, [24]). *A closed subset $\Sigma \subset \mathbb{R}^3$ is called a (positively) invariant region for the initial value problem (23) if any solution $X(x, t)$ with initial values in Σ satisfies $X(x, t) \in \Sigma$ for all $x \in \Omega$ and for all $t \in [0, T_{\max}]$.*

It is well known that rectangular regions are particularly convenient for reaction-diffusion systems. By [24, Corollary 14.8, Theorem 14.11], the hyper-rectangle

$$\Sigma := \left\{ X = (u, v, w) \in \mathbb{R}^3 : a_u \leq u \leq b_u, \quad a_v \leq v \leq b_v, \quad a_w \leq w \leq b_w \right\}$$

is invariant provided the nonlinear mapping F points strictly into Σ on $\partial\Sigma$. If in addition the system (23) has the f -stable property (see [24, Definition 14.10]), it is sufficient that F points non-strictly into Σ on the boundary.

The f -stability of system (23) follows by adapting the proof in [7, Theorem 3]. Thus, it is only necessary to verify that F points inward on the boundary of Σ .

Proof. Let $A_u, A_v, A_w > 0$ denote arbitrary constants, and define the rectangular region

$$\Sigma := \bigcap_{i=1}^3 [0, A_i] \subset \mathbb{R}^3.$$

We introduce the six edge functions

$$G_1(u, v, w) = -u, \quad G_2(u, v, w) = -v, \quad G_3(u, v, w) = -w,$$

$$G_4(u, v, w) = u - A_1, \quad G_5(u, v, w) = v - A_2, \quad G_6(u, v, w) = w - A_3,$$

so that $\Sigma = \bigcap_{j=1}^6 \{G_j \leq 0\}$. By definition, for any boundary point $(u_*, v_*, w_*) \in \partial\Sigma$, there exists a j such that $G_j(u_*, v_*, w_*) = 0$. The condition that the nonlinear mapping F points into Σ is

$$\nabla G_j(u_*, v_*, w_*) \cdot F(u_*, v_*, w_*) \leq 0.$$

If $u_\star = 0$, $v_\star = 0$, or $w_\star = 0$, then $f(u_\star, v_\star, w_\star) = 0$, $g(u_\star, v_\star, w_\star) = 0$, or $h(u_\star, v_\star, w_\star) = 0$ respectively and the condition is satisfied. This already shows that solutions remain nonnegative. On the other hand, if $u_\star = A_1$, or $v_\star = A_2$ or $w_\star = A_3$, then $\nabla G_j = 1$. Using the positivity of u, v, w and the bound $\frac{uv}{1+uv} \leq 1$, the following estimates follow

$$f(A_1, v, w) \leq m_1 - \mu_1 A_1, \quad g(u, A_2, w) \leq m_2 - \mu_2 A_2, \quad h(u, v, A_3) \leq m_3 - \mu_3 A_3.$$

Therefore, by choosing $A_i \geq \eta_i$ for $i = 1, 2, 3$, it holds

$$\nabla G_4(A_1, v, w) \cdot F(A_1, v, w) \leq 0, \quad \nabla G_5(u, A_2, w) \cdot F(u, A_2, w) \leq 0,$$

$$\nabla G_6(u, v, A_3) \cdot F(u, v, A_3) \leq 0.$$

Hence Σ is a bounded invariant region for system (23): any solution starting inside Σ remains inside Σ for all times. So the solution is also bounded, hence global. The proof is complete. \square

(T. André) INSTITUTE FOR MATHEMATICS, HEIDELBERG UNIVERSITY, IM NEUENHEIMER FELD 205, 69120 HEIDELBERG, GERMANY, ORCID.ORG/0009-0001-7320-1941

Email address: theo.andre@uni-heidelberg.de

(S. Cygan) INSTITUTE FOR MATHEMATICS, HEIDELBERG UNIVERSITY, IM NEUENHEIMER FELD 205, 69120 HEIDELBERG, GERMANY, INSTYTUT MATEMATYCZNY, UNIWERSYTET WROCŁAWSKI, PL. GRUNWALDZKI 2/4, 50-384 WROCŁAW, POLAND, ORCID.ORG/0000-0002-8601-829X

Email address: szymon.cygan@uni-heidelberg.de

URL: <http://www.math.uni.wroc.pl/~scygan>

(A. Marciniak-Czochra) INSTITUTE FOR MATHEMATICS AND IWR, HEIDELBERG UNIVERSITY, IM NEUENHEIMER FELD 205, 69120 HEIDELBERG, GERMANY, ORCID.ORG/0000-0002-5831-6505

Email address: anna.marciniak@iwr.uni-heidelberg.de

URL: https://biostruct.iwr.uni-heidelberg.de/folder_people/Anna.Marciniak/index.html

(F. Münnich) INSTITUTE FOR MATHEMATICS, HEIDELBERG UNIVERSITY, IM NEUENHEIMER FELD 205, 69120 HEIDELBERG, GERMANY, ORCID.ORG/0009-0007-9384-2002

Email address: finn.muennich@stud.uni-heidelberg.de